

AD-779 927

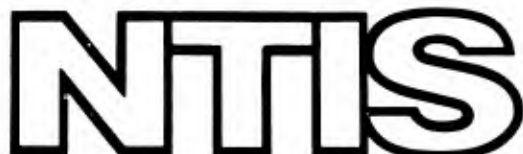
ULTIMATE STRENGTH ANALYSIS OF
SYMMETRIC LAMINATES

R. S. Sandhu

Air Force Flight Dynamics Laboratory
Wright-Patterson Air Force Base, Ohio

February 1974

DISTRIBUTED BY:



National Technical Information Service
U. S. DEPARTMENT OF COMMERCE
5285 Port Royal Road, Springfield Va. 22151

UNCLASSIFIED
Security Classification

AD 779927

DOCUMENT CONTROL DATA - R & D		
(Security classification of title, body of abstract and indexing annotation must be entered when the overall report is classified)		
1. ORIGINATING ACTIVITY (Corporate author) Air Force Flight Dynamics Laboratory Wright-Patterson Air Force Base, Ohio 45433		2a. REPORT SECURITY CLASSIFICATION UNCLASSIFIED
2b. GROUP		
3. REPORT TITLE ULTIMATE STRENGTH ANALYSIS OF SYMMETRIC LAMINATES		
4. DESCRIPTIVE NOTES (Type of report and inclusive dates)		
5. AUTHOR(S) (First name, middle initial, last name) R. S. Sandhu		
6. REPORT DATE February 1974	7a. TOTAL NO. OF PAGES 76	7b. NO. OF REFS 18
8a. CONTRACT OR GRANT NO.	9a. ORIGINATOR'S REPORT NUMBER(S) AFFDL-TR-73-137	
b. PROJECT NO. 4364 c. 436400 d. 43640009	9b. OTHER REPORT NO(S) (Any other numbers that may be assigned this report)	
10. DISTRIBUTION STATEMENT Approved for public release; distribution unlimited		
11. SUPPLEMENTARY NOTES	12. SPONSORING MILITARY ACTIVITY Air Force Flight Dynamics Laboratory Air Force Systems Command Wright-Patterson Air Force Base, Ohio	
13. ABSTRACT A technique is presented for predicting the response to failure of composite laminates. In this technique, cubic spline interpolation functions are used to represent basic stress-strain curves obtained from simple tests. This representation in conjunction with an incremental constitutive law is used to generate response of laminates subjected to incremental loads. The ultimate load-carrying capacity of the laminates is determined by the plywise application of a new failure criterion using strain energy under longitudinal, transverse, and shear loadings as independent parameters. Results obtained by this technique are compared with the available experimental data of boron-epoxy laminates as well as the responses generated by methods of Petit-Waddoups and Hahn. Analytical results determined by the present theory correlate with the experimental data better than those obtained by the other two techniques.		
Reproduced by NATIONAL TECHNICAL INFORMATION SERVICE U S Department of Commerce Springfield VA 22151		

DD FORM 1 NOV 68 1473

UNCLASSIFIED
Security Classification

UNCLASSIFIED
Security Classification

14. KEY WORDS	LINK A		LINK B		LINK C	
	ROLE	WT	ROLE	WT	ROLE	WT
Strength of Laminated Composites						
Failure Criterion						
Biaxial Strength						
Analysis of Composite Laminates						
Nonlinear Analysis						

ia

UNCLASSIFIED
Security Classification

*U.S. Government Printing Office: 1974 — 758-434/557

NOTICE

When Government drawings, specifications, or other data are used for any purpose other than in connection with a definitely related Government procurement operation, the United States Government thereby incurs no responsibility nor any obligation whatsoever; and the fact that the government may have formulated, furnished, or in any way supplied the said drawings, specifications, or other data, is not to be regarded by implication or otherwise as in any manner licensing the holder or any other person or corporation, or conveying any rights or permission to manufacture, use, or sell any patented invention that may in any way be related thereto.

ACCESSION for

NTIS	White Section	<input checked="" type="checkbox"/>
DOC	Doc. Section	<input type="checkbox"/>
UNARMED		<input type="checkbox"/>
JUSTIFICATION		

BY		
DISTRIBUTION/AVAILABILITY CODES		
Block	2000	5000
A		

Copies of this report should not be returned unless return is required by security considerations, contractual obligations, or notice on a specific document.

AFFDL-TR-73-137

ULTIMATE STRENGTH ANALYSIS
OF
SYMMETRIC LAMINATES

R. S. Sandhu

Approved for public release; distribution unlimited

1c

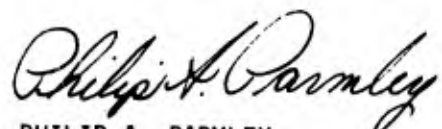
FOREWORD

This work was conducted in the Exploratory Development Group, Advanced Composites Branch, at the Air Force Flight Dynamics Laboratory under Project 4364, "Filamentary Composite Structures."

The author gratefully acknowledges the fruitful discussions he had with Professor Ranbir S. Sandhu, Civil Engineering Department, Ohio State University, Columbus, Ohio, in developing functional representation of stress-strain curves and the failure criterion.

This report was submitted by the author in April 1973.

This technical report has been reviewed and is approved.



PHILIP A. PARMLEY
Chief, Advanced Composites Branch
Structures Division

ABSTRACT

A technique is presented for predicting the response to failure of composite laminates. In this technique, cubic spline interpolation functions are used to represent basic stress-strain curves obtained from simple tests. This representation in conjunction with an incremental constitutive law is used to generate response of laminates subjected to incremental loads. The ultimate load-carrying capacity of the laminates is determined by the plywise application of a new failure criterion using strain energy under longitudinal, transverse, and shear loadings as independent parameters. Results obtained by this technique are compared with the available experimental data of boron-epoxy laminates as well as the responses generated by methods of Petit-Waddoups and Hahn. Analytical results determined by the present theory correlate with the experimental data better than those obtained by the other two techniques.

TABLE OF CONTENTS

SECTION	PAGE
I INTRODUCTION	1
II METHOD OF ANALYSIS	5
III FAILURE CRITERION	13
IV APPLICATIONS	15
1. Unidirectional Laminates	17
2. Off-Axis Coupons	17
3. Angle Ply ($\pm\alpha^\circ$) Laminates	29
4. Cross Ply (0°/90°) Laminates	35
5. (0°/ $\pm\alpha^\circ$) _s Laminates	40
6. Multidirectional Laminates	51
V DISCUSSION OF RESULTS AND CONCLUSIONS	72
REFERENCES	74

ILLUSTRATIONS

FIGURE	PAGE
1 Strain (ϵ_2) Under Biaxial Stress Field (σ_1, σ_2)	8
2 Transformation of Axes	10
3 Comparison of Various Strength Theories	16
4 Lamina Shear Response	19
5 Lamina Transverse Tension Response	20
6 Boron-Epoxy 15° Off-Axis Coupon	22
7 Boron-Epoxy 30° Off-Axis Coupon	23
8 Boron-Epoxy 45° Off-Axis Coupon	24
9 Boron-Epoxy 60° Off-Axis Coupon	25
10 Boron-Epoxy 75° Off-Axis Coupon	26
11 Percentage Contribution to Degradation of Off-Axis Specimens	27
12 Failed Off-Axis Coupons	30
13 Response of ($\pm 45^\circ$) Laminate Subjected to Stress σ_x only	31
14 Response of ($\pm 30^\circ$) Laminate Subjected to Stress σ_x only	32
15 Response of ($\pm 60^\circ$) Laminate Subjected to Stress σ_x only	33
16 Percentage Contribution to Degradation of ($\pm \alpha^\circ$) Laminates Subjected to Stress σ_x only	34
17 Strength Envelope for ($\pm 45^\circ$) Laminate	36
18 Strength Envelopes for ($\pm \alpha^\circ$) Laminates	37
19 Strength Envelope for ($0^\circ/90^\circ$) Laminate	41
20 Percentage Contribution to Degradation of ($0^\circ/90^\circ$) Laminate Subjected to Various Stress Ratios	42

ILLUSTRATIONS (CONT)

FIGURE	PAGE
21 Stress-Strain Response of $(0^\circ/90^\circ)$ Laminate Subjected to a Stress Ratio, $\sigma_x/\sigma_y = 0:1$	43
22 Stress-Strain Response of $(0^\circ/90^\circ)$ Laminate Subjected to a Stress Ratio, $\sigma_x/\sigma_y = 1:2$	44
23 Stress-Strain Response of $(0^\circ/90^\circ)$ Laminate Subjected to a Stress Ratio, $\sigma_x/\sigma_y = 1:1$	45
24 Stress-Strain Response of $(0^\circ/90^\circ)$ Laminate Subjected to a Stress Ratio, $\sigma_x/\sigma_y = -1:1$	46
25 Strength Envelope for $(0^\circ/\pm 60^\circ)_s$ Laminate	47
26 Percentage Contribution to Degradation of $(0^\circ/\pm 60^\circ)_s$ Laminate Subjected to Various Stress Ratios	48
27 Stress-Strain Response of $(0^\circ/\pm 60^\circ)_s$ Laminate Subjected to Stress σ_x only	49
28 Stress-Strain Response of $(0^\circ/\pm 60^\circ)_s$ Laminate Subjected to Stress σ_y only	50
29 Strength Envelope for $(0^\circ/\pm 45^\circ)_s$ Laminate	52
30 Percentage Contribution to Degradation of $(0^\circ/\pm 45^\circ)_s$ Laminate Subjected to Various Stress Ratios	53
31 Strength Envelope for $(0^\circ/\pm 45^\circ/90^\circ)_s$ Laminate	56
32 Percentage Contribution to Degradation of $(0^\circ/\pm 45^\circ/90^\circ)_s$ Laminate Subjected to Various Stress Ratios	57
33 Stress-Strain Response of $(0^\circ/\pm 45^\circ/90^\circ)_s$ Laminate Subjected to Stress σ_y only	58
34 Stress-Strain Response of $(0^\circ/\pm 45^\circ/90^\circ)_s$ Laminate Subjected to a Stress Ratio, $\sigma_x/\sigma_y = 1:2$	59
35 Stress-Strain Response of $(0^\circ/\pm 45^\circ/90^\circ)_s$ Laminate Subjected to a Stress Ratio, $\sigma_x/\sigma_y = 1:1$	60

ILLUSTRATIONS (CONT)

FIGURE	PAGE
36 Stress-Strain Response of $(0^\circ/\pm 45^\circ/90^\circ)_s$ Laminate Subjected to a Stress Ratio, $\sigma_x/\sigma_y = -1:2$	61
37 Strength Envelope for $(0^\circ_2/\pm 45^\circ/90^\circ)_s$ Laminate	65
38 Percentage Contribution to Degradation of $(0^\circ_2/\pm 45^\circ/90^\circ)_s$ Laminate Subjected to Various Stress Ratios	66
39 Strength Envelope for $(0^\circ/\pm 45^\circ/0^\circ/90^\circ)_s$ Laminate	68
40 Percentage Contribution to Degradation of $(0^\circ/\pm 45^\circ/0^\circ/90^\circ)_s$ Laminate Subjected to Various Stress Ratios	69
41 Strength Envelopes of $(0^\circ/\pm 45^\circ/90^\circ)_c$ Laminates	70

TABLES

TABLE	PAGE
I Strength and Degradation of Off-Axis Coupons	28
II Failure Stress for $(\pm\alpha^\circ)$ and $(0^\circ/90^\circ)$ Laminates	38
III Degradation of $(\pm\alpha^\circ)$ and $(0^\circ/90^\circ)$ Laminates	39
IV Failure Stresses and Percentage Degradation for $(0^\circ/\pm 60^\circ)_s$ Laminates	54
V Failure Stresses and Percentage Degradation for $(0^\circ/\pm 45^\circ)_s$ Laminates	55
VI Failure Stresses and Percentage Degradation of $(0^\circ/\pm 45^\circ/90^\circ)_s$ Laminate	62
VII Failure Stresses and Percentage Degradation of $(0^\circ_2/\pm 45^\circ/90^\circ)_s$ Laminate	63
VIII Failure Stresses and Percentage Degradation of $(0^\circ/\pm 45^\circ/0^\circ/\overline{90^\circ})_s$ Laminate	64
IX Analytical-Experimental Strengths of $(0^\circ/\pm 45^\circ/0^\circ/\overline{90^\circ})_s$ Laminate	71

SECTION I

INTRODUCTION

Filamentary composite laminates are being used in aircraft structural components in increasing numbers. To use these materials satisfactorily we need to know their stress-strain behavior and ultimate strength under design loads. This data can be obtained experimentally, but this is both expensive and inconvenient, since a large variety of laminates can be fabricated from basic unidirectional plies. The other technique would be to analytically relate the properties of the lamina to those of the laminate. This would require knowing the material biaxial properties of the lamina for various load combinations, which information is not available at present.

Presently properties of the lamina under simple loading conditions (uniaxial tension, uniaxial compression, and pure shear) may either be estimated from the properties of its constituents (Reference 1) or determined experimentally. The estimation procedure has not proved effective, so mechanical properties of the lamina are obtained by tests. The behavior of the lamina under complex stress states is predicted by using some criterion to relate the parameters of strength obtained from simple tests to the stress states. In this technique we normally assume that the yield stress and the ultimate strength are synonymous. Some of these failure theories (Reference 2) assume an interaction between the failure modes to generate a smooth failure surface. Others treat the failure modes as being independent.

Even if the behavior of the lamina can be accurately predicted, the problem of determining the performance of laminas in a laminate still remains. The degradation of strength of individual laminas may not precipitate failure of the laminate. For example, in the case of a cross ply ($0^\circ/90^\circ$) laminate subjected to normal stresses (σ_1, σ_2) acting in the direction of the fibers, the degradation of strength of laminas in the transverse direction does not result in the failure of the

laminate; it is capable of sustaining stresses higher than those causing transverse degradation of the individual laminas.

This lamina-laminate response has been a subject of many theoretical and experimental studies. Tsai (Reference 3) assumed the lamina to be quasi-homogeneous, orthotropic, and linearly elastic to failure, and he determined stress states in all plies due to applied loads. To satisfy Hill's failure criterion, the plies were considered to be degraded and their stiffnesses modified; however, in this technique, the exact nature of degradation is not explicitly defined. Later Tsai, et al (Reference 4) to account for post yielding behavior of the laminate, proposed a new technique incorporating some of the assumptions of netting analysis. After initial degradation, this technique postulates that the laminate can sustain stresses in the direction of fibers, which is made possible by the assumption that an internal agency exists. This agency would provide resistance to the externally applied loads by developing axial loads along the fibers.

Noyes and Jones (Reference 5) extended the concepts of Reference 3 by modifying Hill's criterion to determine the onset of failure in a ply or plies. To determine the associated failure mode, they proposed an empirical technique based upon inequalities involving the stress state and parameters of strength. If the analysis indicates a transverse or a shear failure mode, both the transverse and the shear stiffnesses of the affected plies are set to zero; with longitudinal failure, all the stiffnesses are reduced to zero. The loading is continued with the remaining plies intact until general failure of the laminate. This procedure assumes instantaneous failure of the plies; however, the failure may be gradual with loading rather than instantaneous. Chiu (Reference 6) suggested the approach by Noyes and Jones be modified to reduce the affected stiffnesses and strengths gradually.

All the above approaches assumed linearity of lamina stress-strain relations. Petit and Waddoups (Reference 7) relaxed this restriction; to determine response of the laminates, they used properties of unidirectional laminae in conjunction with a piece-wise linear approach.

The loading is proportional and is applied in small increments to compute corresponding strain increments. These increments are added to the previous strains to obtain the resultant strains at a particular load level. These strains are used to determine the elastic constants to be used in the next cycle. When strain components reach limiting values, lamina or laminae are assumed to unload rapidly, thereby transferring their share of load to the intact layers. The laminate fails when it cannot sustain any more load increments. Tangent moduli are obtained from stress-strain curves using the lamina strains; however, this does not consider the fact that the strains in the input stress-strain curves are simple, while the lamina strains in the laminate are not. (This aspect will be discussed in greater detail in Section II.) Additionally, stress-strain curves of laminates obtained by this method are very much dependent upon the size of the increment used in the applied loads.

Recently a new technique (References 8 and 9) has been proposed for the study of the nonlinear behavior of laminated composites. This technique incorporates only nonlinearity of shear, represented by the equation

$$\epsilon_6 = S_{66} \sigma_6 + S_{6666} \sigma_6^3 \quad (1)$$

where σ_6, ϵ_6 are shear stress and shear strain, respectively, and S_{66}, S_{6666} are constants. This approach does not distinguish between tension and compression behaviors, however, and it does not deal with the problem of failure.

This report describes a technique using cubic spline interpolation functions to represent the basic stress-strain data, namely,

- a. Longitudinal tension and compression,
- b. Transverse tension and compression, and
- c. Shear.

This functional form of stress-strain curves provides an accurate representation of stresses, strains, and moduli over the entire range of the curves. The incremental constitutive law relates the increments of

stresses and strains. The basic data and the constitutive relations are used to determine the ultimate cumulative response of the laminates under incremental loading by a new failure criterion. This criterion is based upon the concept that strain energies under longitudinal, transverse, and shear loadings are independent parameters. The analytical response obtained by the three methods (the proposed technique and those of References 7 and 8 and 9) is compared with the available boron-epoxy experimental results.

SECTION II

METHOD OF ANALYSIS

The basic constituent of a laminate is a unidirectional lamina or ply. This lamina is essentially orthotropic. The mechanical properties of the lamina under static loads are determined by conducting five simple tests (uniaxial tension and compression along and transverse to the material axes and shear). Generally, these tests indicate a nonlinear behavior of the lamina. For this reason, an incremental type constitutive law is desirable to define the response of the lamina under general states of stress. To define the general incremental constitutive relationship, it is assumed that

- a. The increment of strain depends upon the strain state and the increment of stress; and
- b. The increment of strain is proportional to the increment of stress.

Using the above assumptions, the incremental constitutive law can be written as

$$d\epsilon_{ij} = S_{ijrs}(\epsilon_{ij}) d\sigma_{rs} \quad (i, j, r, s = 1, 2, 3) \quad (2)$$

where $d\epsilon_{ij}$, $d\sigma_{rs}$ are strain and stress increments and S_{ijrs} is a function of the current strains, ϵ_{ij} .

The incremental constitutive relation using contracted notation for the lamina under generalized plane stress reduces to

$$d\epsilon_i = S_{ij}(\epsilon_i) d\sigma_j \quad (i, j = 1, 2, 6) \quad (3)$$

Equation 3 written explicitly becomes

$$\begin{bmatrix} d\epsilon_1 \\ d\epsilon_2 \\ d\epsilon_6 \end{bmatrix} = \begin{bmatrix} S_{11} & S_{12} & S_{16} \\ S_{21} & S_{22} & S_{26} \\ S_{61} & S_{62} & S_{66} \end{bmatrix} \begin{bmatrix} d\sigma_1 \\ d\sigma_2 \\ d\sigma_6 \end{bmatrix} \quad (4)$$

or simply

$$[d\epsilon] = [S] [d\sigma] \quad (5)$$

where $d\sigma_1$, $d\epsilon_1$ = normal stress and strain increments in the fiber direction,

$d\sigma_2$, $d\epsilon_2$ = normal stress and strain increments in the transverse direction,

$d\sigma_6$, $d\epsilon_6$ = shear stress and strain increments

S_{11} , S_{12} , etc. = elements of compliance matrix representing the average values during the increment of stresses.

Since the lamina is assumed to remain orthotropic at all load levels, the elements

$$S_{16} = S_{26} = S_{61} = S_{62} = 0 \quad (6)$$

$$\left. \begin{array}{l} S_{11} = 1/E_{11} ; S_{22} = 1/E_{22} ; S_{66} = 1/G_{12} \\ S_{12} = S_{21} = -\nu_{12}/E_{11} = -\nu_{21}/E_{22} \end{array} \right\} \quad (7)$$

Combining Equations 4, 6, and 7 provides incremental stress-strain relations for the lamina

$$d\epsilon_1 = d\sigma_1 (1 - \nu_{12} B) / E_{11} \quad (8)$$

$$d\epsilon_2 = d\sigma_2 (1 - \nu_{21}/B) / E_{22} \quad (9)$$

$$d\epsilon_1 = d\sigma_1 / G_{12} \quad (10)$$

where

$$B = d\sigma_2 / d\sigma_1 \quad (11)$$

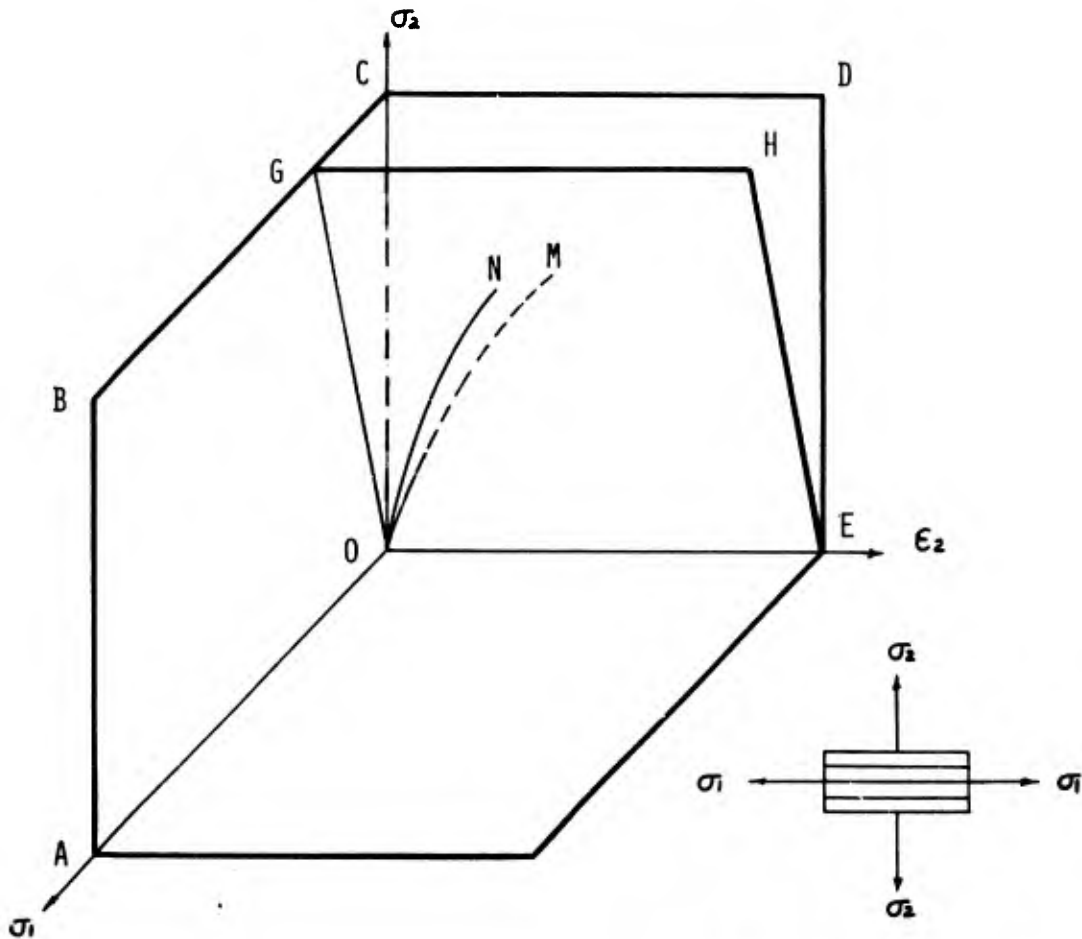
Equations 8 and 9 reveal that it would be erroneous to use $d\epsilon_1$ or $d\epsilon_2$ representing the biaxial stress state $d\sigma_1, d\sigma_2$ to determine E_{11} or E_{22} from stress strain curves obtained under simple loading conditions. For example, $d\epsilon_2$ of Equation 9 corresponds to the curve ON (Figure 1) on the plane OEHG while the simple stress strain curve OM lies on the plane OEDC. Since stress-strain data similar to ON is not available, we have assumed that simple equivalent strain increments can be computed from the following expressions:

$$d\epsilon_1 \Big|_{\text{Eq.}} = d\epsilon_1 / (1 - \nu_{12} B) \quad (12)$$

$$d\epsilon_2 \Big|_{\text{Eq.}} = d\epsilon_2 / (1 - \nu_{21} / B) \quad (13)$$

In the application of the incremental constitutive law to multi-directional laminates, Equation 5 for the k-th ply is written as

$$[\mathbf{d}\sigma]_k = [\mathbf{C}]_k [\mathbf{d}\epsilon]_k \quad (14)$$



$$\epsilon_2 = \sigma_2 (1 - \nu \sigma_1 / \sigma_2) / E_2$$

Figure 1. Strain (ϵ_2) Under Biaxial Stress Field (σ_1, σ_2)

where

$$[C]_k = [S]_k^{-1} = \text{Stiffness matrix of } k\text{-th ply}$$

$$[d\sigma]_k = \text{Stress increment in the } k\text{-th ply relative to the material axes 1, 2}$$

$$[d\epsilon]_k = \text{Strain increment in the } k\text{-th ply relative to the material axes 1, 2}$$

In the case of multidirectional laminates, load axes X, Y generally do not coincide with the material axes 1, 2 (Figure 2). Stress and strain increments in two coordinate systems are related by a transformation matrix $[T]_k$, i.e.,

$$[d\sigma]_k = [T]_k [d\bar{\sigma}]_k \quad (15)$$

$$[d\epsilon]_k = [T]_k [d\bar{\epsilon}]_k \quad (16)$$

where $[d\bar{\sigma}]_k$ and $[d\bar{\epsilon}]_k$ are the stress and strain increments in the X, Y coordinate system. Substitution of Equations 15 and 16 in 14, yields

$$\begin{aligned} [T]_k [d\bar{\sigma}]_k &= [C]_k [T]_k [d\bar{\epsilon}]_k \\ [d\bar{\sigma}]_k &= [T]_k^{-1} [C]_k [T]_k [d\bar{\epsilon}]_k \\ &= [\bar{C}]_k [d\bar{\epsilon}]_k \end{aligned} \quad (17)$$

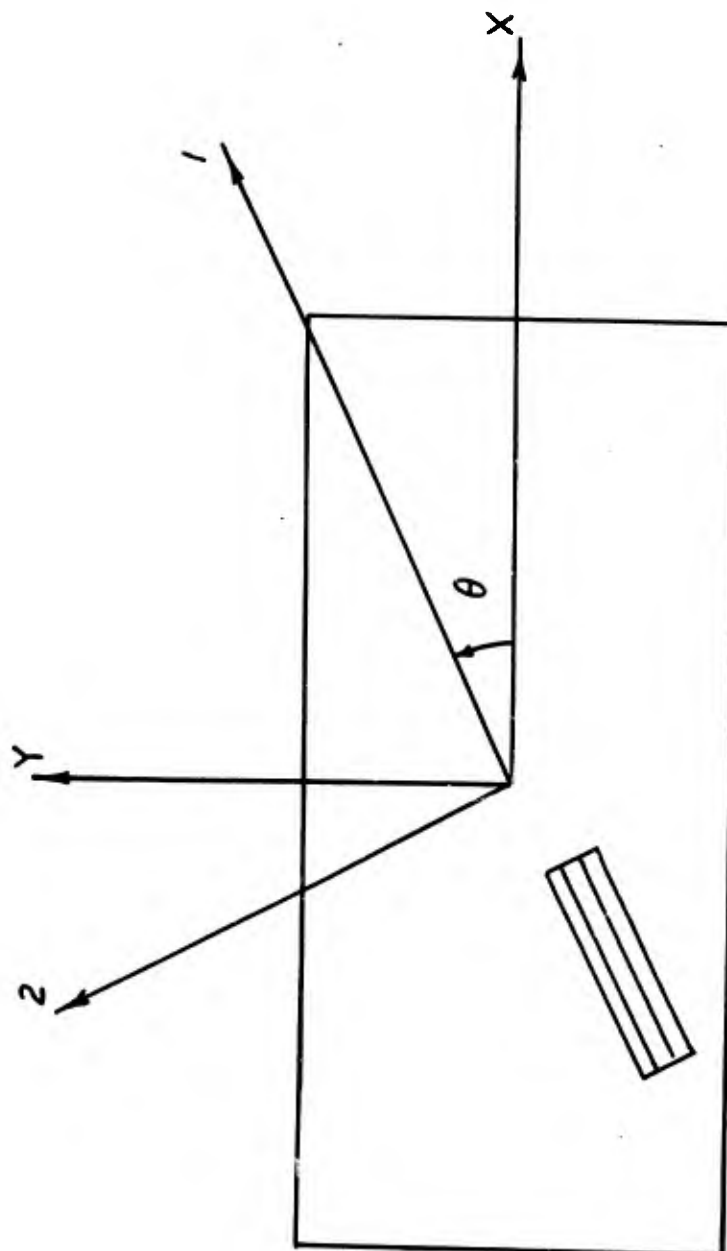


Figure 2. Transformation of Axes

where

$$[\bar{C}]_k = [T]_k^{-1} [C]_k [T]_k \quad (18)$$

Assuming that stresses are uniformly distributed through the thickness of each ply, stress resultant increments $[dN]$, in the X, Y coordinate system are given by

$$[dN] = \sum_{k=1}^p [d\bar{\sigma}]_k t_k \quad (19)$$

t_k = thickness of k-th ply

p = number of plies in a laminate

On substituting Equation 17 in Equation 19, stress resultant increments become

$$[dN] = \sum_{k=1}^p t_k [\bar{C}]_k [d\bar{\epsilon}]_k \quad (20)$$

Assuming that the strain increments $[d\bar{\epsilon}]_k$ are the same for all plies of the laminate, i.e.,

$$[d\bar{\epsilon}]_k = [d\bar{\epsilon}] \quad (21)$$

Equation 20 becomes

$$[dN] = [A] [d\bar{\epsilon}] \quad (22)$$

where

$$[A] = \sum_{k=1}^p t_k [\bar{C}]_k \quad (23)$$

Inversion of Equation 22 yields

$$[\delta\epsilon^o] = [A]^{-1} [dN] \quad (24)$$

In Equation 24 $[A]^{-1}$ represents the average compliance properties of the laminate during the $(n+1)$ th load increment. However, $[A]^{-1}$ is not known when $(n+1)$ th load increment is applied. To overcome this difficulty elastic properties at the end of the n th load increment are used in Equation 24, i.e.,

$$[\delta\epsilon^o]_{n+1} = [A]_n^{-1} [dN]_{n+1} \quad (25)$$

The strain increments $[\delta\epsilon^o]_{n+1}$ obtained from Equation 25 are used in Equations 17, 15, 16, 12, and 13 to calculate $[\delta\sigma]_k$, $[\delta\epsilon]_k$, $\delta\epsilon_1|_{\text{Eq.}}$ and $\delta\epsilon_2|_{\text{Eq.}}$. These stress and strain increments are added to Eq. stresses and strains at the n th load increment to obtain the current stresses and strains in all plies. The current stresses and strains are employed to determine the average elastic properties of the plies and a new $[A]^{-1}$ is computed. This procedure is repeated till the difference between two values of $[\delta\epsilon^o]_{n+1}$ in two consecutive cycles is small to the order of approximation desired. The Equation 25, then becomes

$$[\delta\epsilon^o]_{n+1} = [A]_{n+1}^{-1} [dN]_{n+1} \quad (26)$$

The repetitive use of the procedure outlined above generates the stress-strain response of multidirectional laminates.

SECTION III

FAILURE CRITERION

The incremental loading procedure outlined in Section I, to predict the response of the laminate, cannot proceed indefinitely. A stage is reached where a lamina or laminas can no longer sustain additional loads. The failure state of the lamina under general stress states is determined by a criterion relating its behavior to that under simple load conditions. In the formulation of the criterion for anisotropic materials, essentially two approaches (Reference 2) have been used. One approach characterizes the failure state to be when stress/strain components exceed the limit obtained by simple tests. The second approach has been to use different quadratic forms of stresses with or without linear terms to establish the failure state. The coefficients of the quadratic expression are evaluated by using results of simple or both simple and biaxial tests. These approaches assume that yield and ultimate states are analogous. For materials exhibiting nonlinear response under loading, the two states are not the same, and the failure state would be a function of both stress and strain states.

A scalar function, f , defining the failure condition of materials exhibiting nonlinear behavior can be written as

$$f(\sigma, \epsilon, K) = 1 \quad (27)$$

where σ, ϵ are the stress strain states and K is the material characteristics.

An explicit form of Equation 27 proposed in this report uses the scalar strain energy as a measure to determine the level of the effect of both stress and strain states on the material behavior. Assuming strain energies as independent parameters, the failure criterion for orthotropic materials may be expressed as

$$K_{ij} \left[\int_{\epsilon_{ij}} \sigma_{ij} d\epsilon_{ij} \right]^m = 1 \quad (i, j = 1, 2, 3) \quad (28)$$

where ϵ_{ij} are the current strain components and m is a parameter defining the shape of the failure surface in the strain energy space. The failure criterion (Equation 28) is based upon total strain energies. It includes the effect of hydrostatic loading. This inclusion, according to Reference 10, is necessary to allow for the heterogeneous deviatoric stress field caused in fiber-reinforced composites by the hydrostatic loading. In case of anisotropic materials which are not influenced by the hydrostatic loading, an equation similar to Equation 28 can be written in terms of energies of distortion.

Equation 28, using contracted notation, specialized for the plane stress condition becomes

$$K_i \left[\int_{\epsilon_i} \sigma_i d\epsilon_i \right]^m = 1 \quad (i = 1, 2, 6) \quad (29)$$

Using the results of tests under simple load conditions

$$K_i = \left[\int_{\epsilon_{iu}} \sigma_i d\epsilon_i \right]^m \quad (i = 1, 2, 6) \quad (30)$$

where ϵ_{1u} , ϵ_{2u} and ϵ_{6u} are the ultimate normal (tensile or compressive) and shear strains. Combining Equations 29 and 30, the following equation is obtained

$$\left[\int_{\epsilon_i} \sigma_i d\epsilon_i \Big/ \int_{\epsilon_{iu}} \sigma_i d\epsilon_i \right]^m = 1 \quad (i = 1, 2, 6) \quad (31)$$

The shape of the failure surface (Equation 31) in the strain energy space is determined by the shape factor, m ; for $m = 2$, it is spherical and for $m = 1$, it is pyramidal.

SECTION IV

APPLICATIONS

A computer program embodying the concepts of Sections II and III was developed to determine the theoretical responses of laminates subjected to in-plane loads to compare them with the available experimental data. This analytical-experimental correlation was confined to data for the boron-epoxy material system. The basic property data (results of simple tests) of the boron-epoxy material system needed for the computer program was extracted from Reference 11. In the application of the technique, cubic spline interpolation functions (References 12 and 13) were used to represent the basic stress-strain data of laminas. This functional form of stress-strain curves provides a much better representation of the stress-strain curves and moduli over the entire range of the curve than the two or three parameter mathematical function or the piecewise linear approach used in References 7 to 9.

In addition to a suitable representation of nonlinearity of the basic stress-strain curves, the criterion defined in Section III was used to determine the ultimate cumulative response of laminates subjected to incremental loads. The criterion for three values of the parameter m , namely $m = 1/2$, 1, and 2, was compared with some of the other failure theories in the first quadrant of the stress space in Figure 3. The choice of the value of the shape factor m for a material system depends upon the ability of the criterion to match the experimental results. At present there is no reliable experimental data of boron-epoxy unidirectional laminas under biaxial stress states, which could be used to determine a suitable value of m . However, in case of multidirectional laminates a better corroboration between experimental and analytical results was observed for $m = 1$. For this reason the parameter m was taken to be unity for the study reported herein. With $m = 1$ the criterion reduces to the maximum strain energy theory for linearly elastic and isotropic materials.

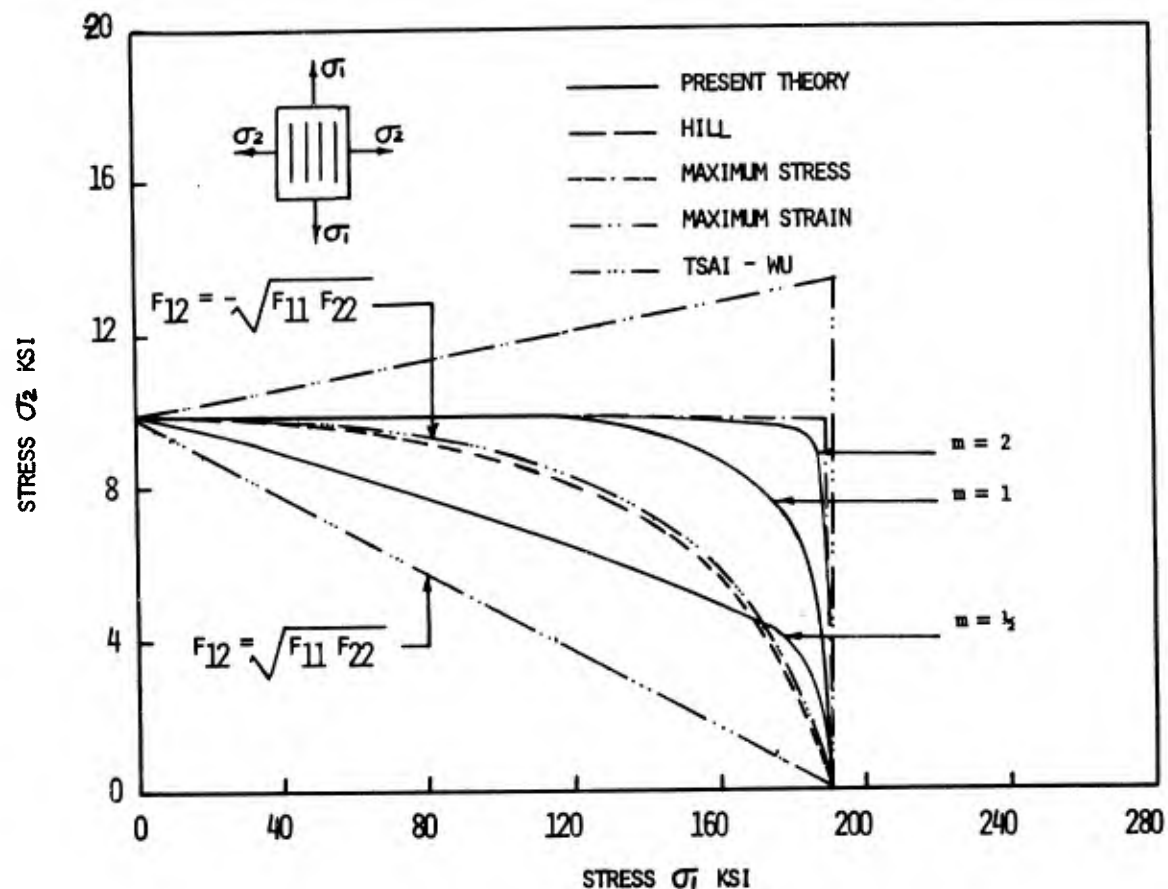


Figure 3. Comparison of Various Strength Theories

The hypothesized criterion assumes strain energies under longitudinal, transverse, and shear loading as independent parameters. When the sum of three ratios of the current energy level to the available one equals unity the lamina degrades completely (Equation 31). The three terms of Equation 31 at the time of failure represent contributions to degradation made by longitudinal, transverse, and shear stresses acting on the laminas. In application to multidirectional laminates, the criterion is satisfied plywise. When the contribution to degradation is dominantly transverse or shear and characterized by matrix failure mode, the lamina is assumed to be capable of sustaining longitudinal loads.

The incremental constitutive law in conjunction with the failure criterion was used to predict the response of various boron-epoxy laminates. To compare the predictions with the available experimental data, we examined four categories of symmetric laminates:

- (a) Unidirectional laminates including off-axis coupons
- (b) Angle Ply ($+\alpha$) laminates;
- (c) ($0/\pm\alpha$) laminates; and
- (d) Multidirectional laminates.

1. UNIDIRECTIONAL LAMINATES

At present the technology to test (0°) laminates under biaxial stress states is not sufficiently advanced to yield reliable data. In the absence of relevant data, no analytical-experimental corroboration for these laminates was feasible.

2. OFF-AXIS COUPONS

In the case of off-axis coupons, the laminates are unidirectional but the load axis and the material axes do not coincide. This creates a biaxial stress state relative to the material axes. Gripping and test techniques being employed tend to introduce nonuniform stress states

within the test section of the coupon. With a large aspect ratio (length/width > 10), however, a fairly uniform stress field develops at the midsection of the coupon. The aspect ratio between specimen tabs used in the experimental program (Reference 14) from which this data was extracted was 16. The specimens were 0.5 inch wide.

In developing the incremental constitutive relations in Section II, we assumed that the lamina was orthotropic in its behavior. To substantiate this, we measured the stresses and strains under tensile loadings of off-axis coupons relative to the material axes; these values are plotted in Figures 4 and 5, along with simple stress-strain curves obtained from Reference 11. The resolved stress-strain curves are close to the curves obtained under simple load conditions, which indicates that there is practically no coupling between normal and shearing deformations. This leads to the conclusion that the lamina does tend to retain its orthotropic characteristics to failure. In the absence of similar data under compressive loading, we assume the behavior of the lamina would be similar.

Stress-strain curves of 15°, 30°, 45°, and 60°, and 75° off-axis coupons obtained experimentally (Reference 14) and using analytical techniques are shown in Figures 6 to 10. Of the three analytical curves, one is based upon the theory presented in this report and the other two on the concepts of References 7 and 8. The analytical curve based on Reference 7 is very much dependent upon the size of the increment of the load. The attempt to represent curved segments of the basic stress-strain curves by a series of line segments introduces errors which are cumulative. Additionally the ultimate cumulative response, according to this technique, is attained when any of the strain components associated with the material axes reaches the limiting value. On the other hand, the analytical curve based upon Reference 8 is not dependent upon the size of the load increment, but it makes no attempt to determine the ultimate response. This analysis assumes that only the shear stress-strain behavior of the lamina is nonlinear. Equation 1 can approximate the curve by matching the slope at the origin and making it pass through some other convenient point.

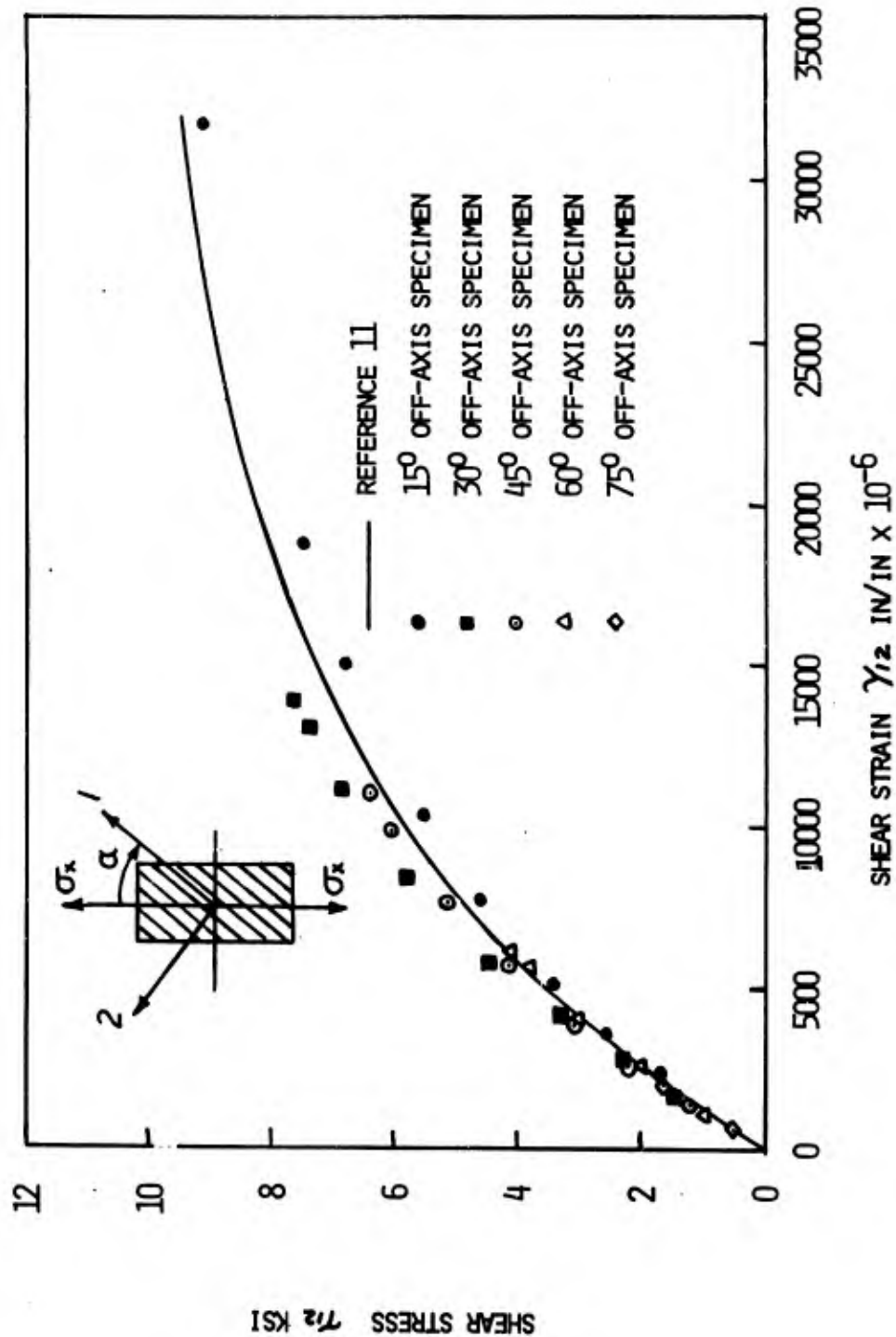


Figure 4. Lamina Shear Response

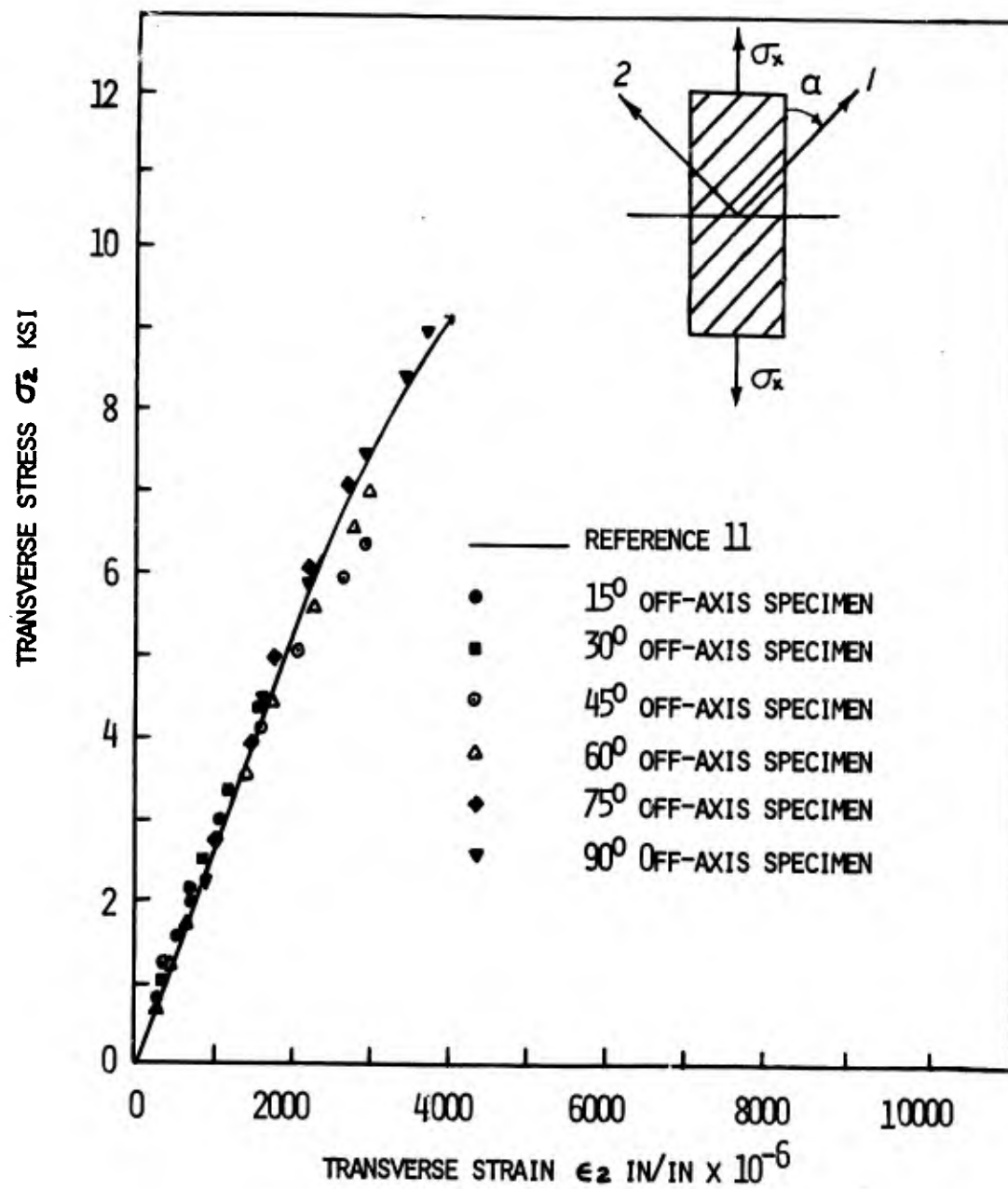


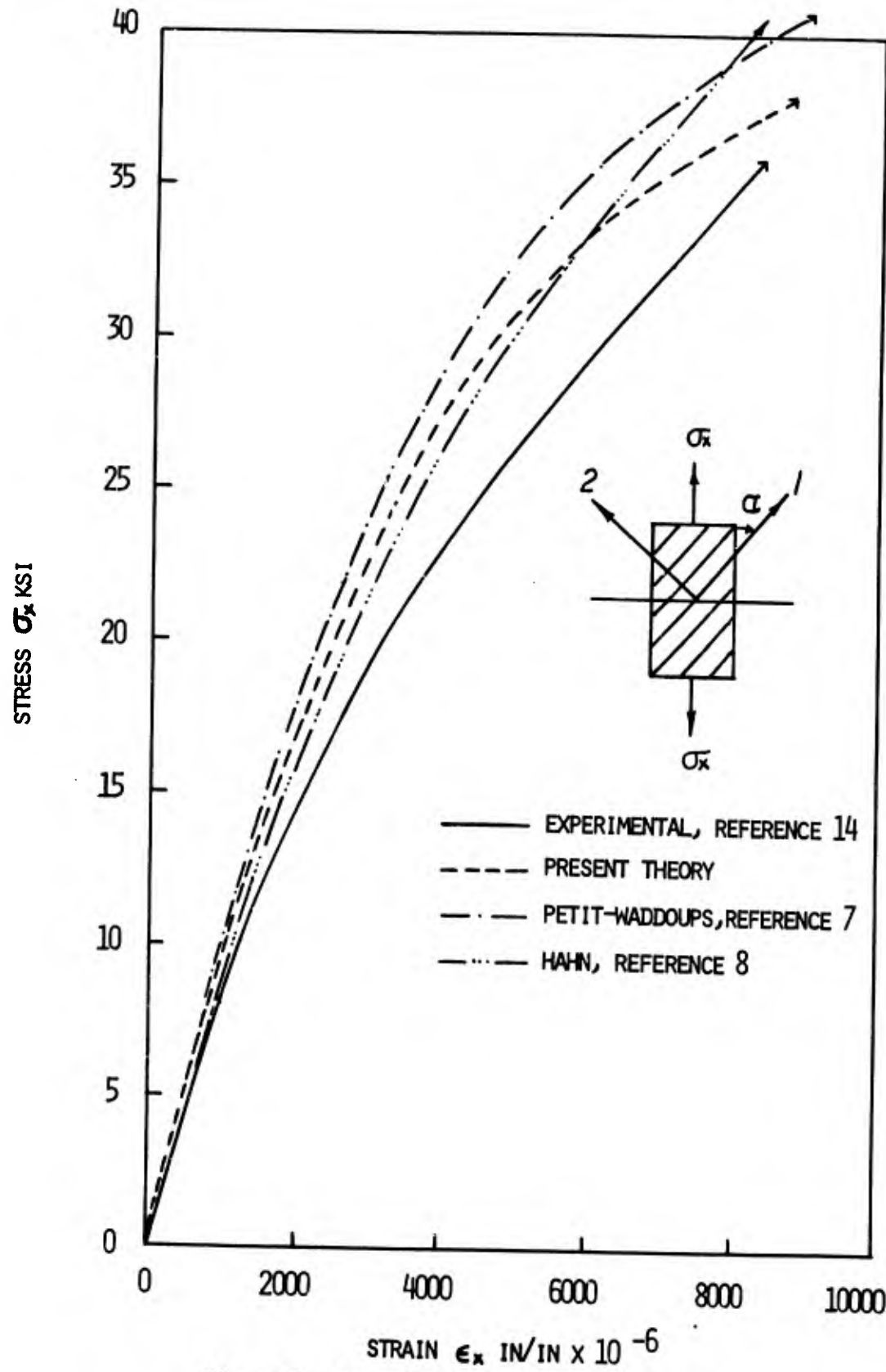
Figure 5. Lamina Transverse Tension Response

The response of the 15° off-axis coupon (Figure 6) is governed mainly by the lamina shear stress-strain response, which contributes 94.14% to the degradation of the coupon (Table I and Figure 11). The stiffer shear stress-strain response of the lamina as compared to that of the 15° coupon (Figure 4) is reflected in the difference between the analytical and the experimental behavior. The reasons for the differences in the analytical curves were discussed earlier.

With increasing orientation of fibers, the effect of the transverse stress-strain response of the lamina on the behavior of off-axis coupons increases, but the shear effect diminishes. For an orientation angle greater than 60°, the transverse effect contributes more than 87.97% to the failure. In this case the analytical curves based upon Reference 8, which do not consider the nonlinearity of the transverse stress-strain response of the lamina, depart more from the experimental behavior. Experimental stress-strain curves agree better with the analytical responses obtained using the concepts of this report than with those of either Reference 7 or Reference 8. However, experimental and predicted strengths tend to diverge with increasing orientation especially for $\alpha > 45^\circ$. This may well be due to such factors as nonuniformity of stresses in the test section, the width-effect of the specimens (0.5" wide specimens were used in the test program), residual stresses, etc.

Theoretical strengths and the contributions to degradation for various orientations of fibers in off-axis coupons are presented in Table I. Percentages contributions to degradation of off-axis coupons are shown in Figure 11. The theoretical curves in Figure 11 indicate that

- (a) For α greater than 7°, matrix failure mode dominates;
- (b) For $\alpha = 10^\circ$ to 20° , failure is essentially shear type;
- (c) For $\alpha = 20^\circ$ to 60° , failure is a combination of transverse and shear modes;
- (d) For α greater than 60°, failure is a transverse one.



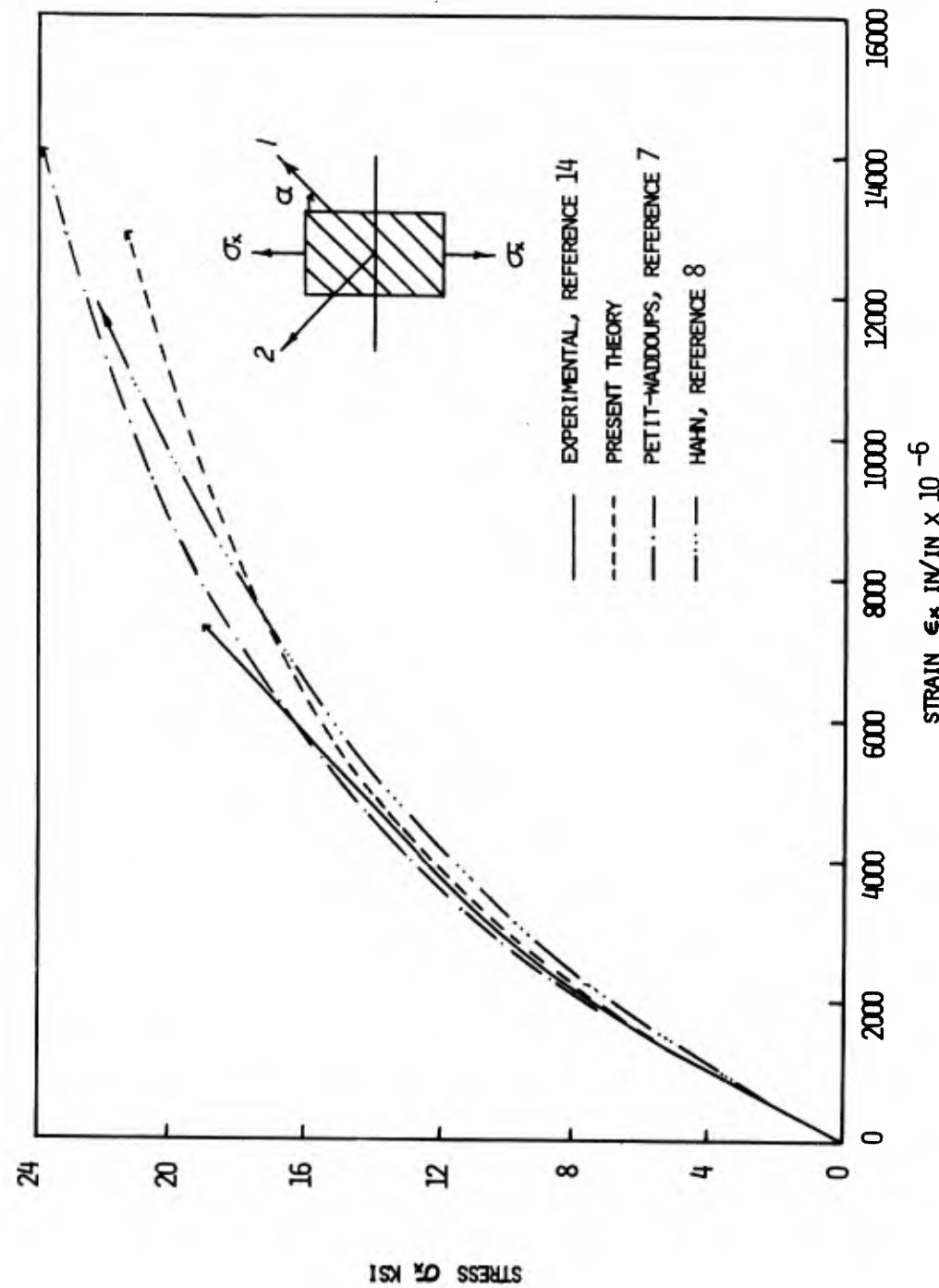


Figure 7. Boron-Epoxy 30° Off-Axis Coupon

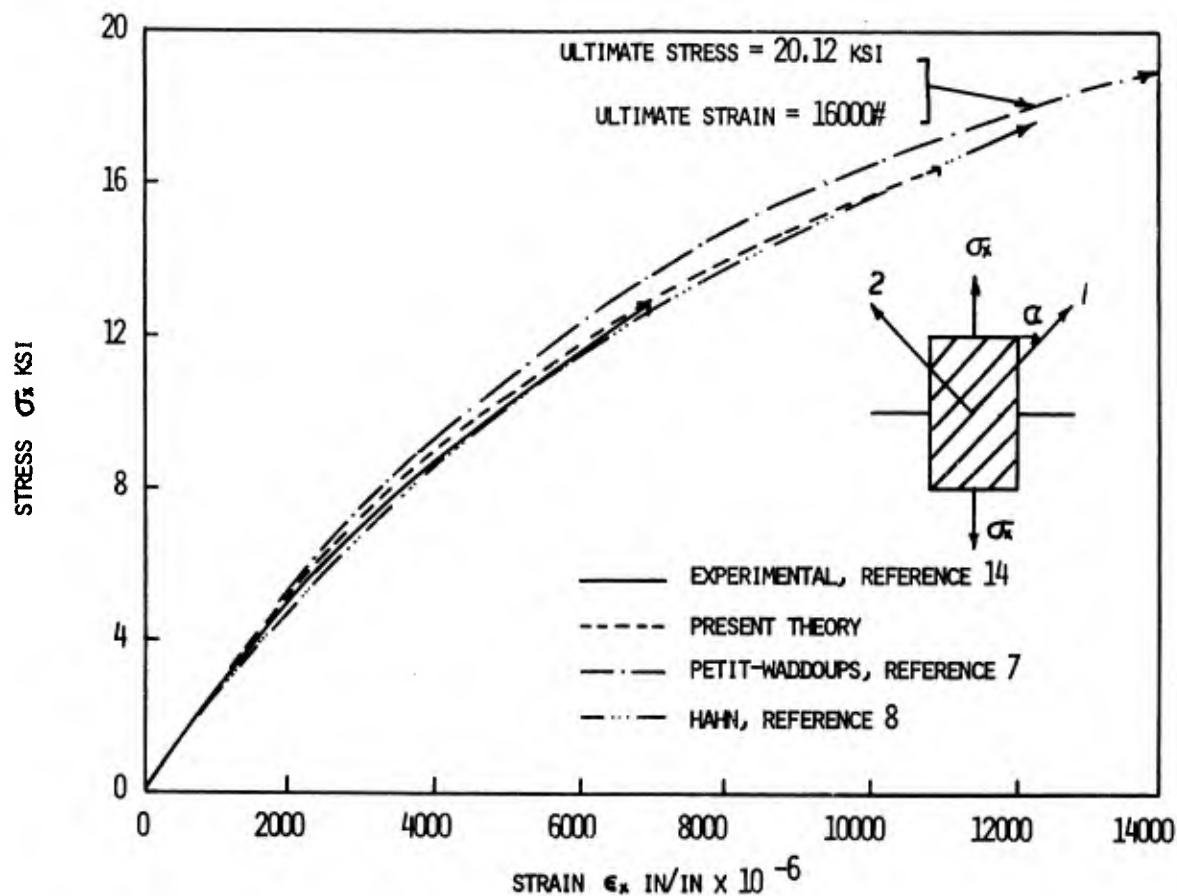


Figure 8. Boron-Epoxy 45° Off-Axis Coupon

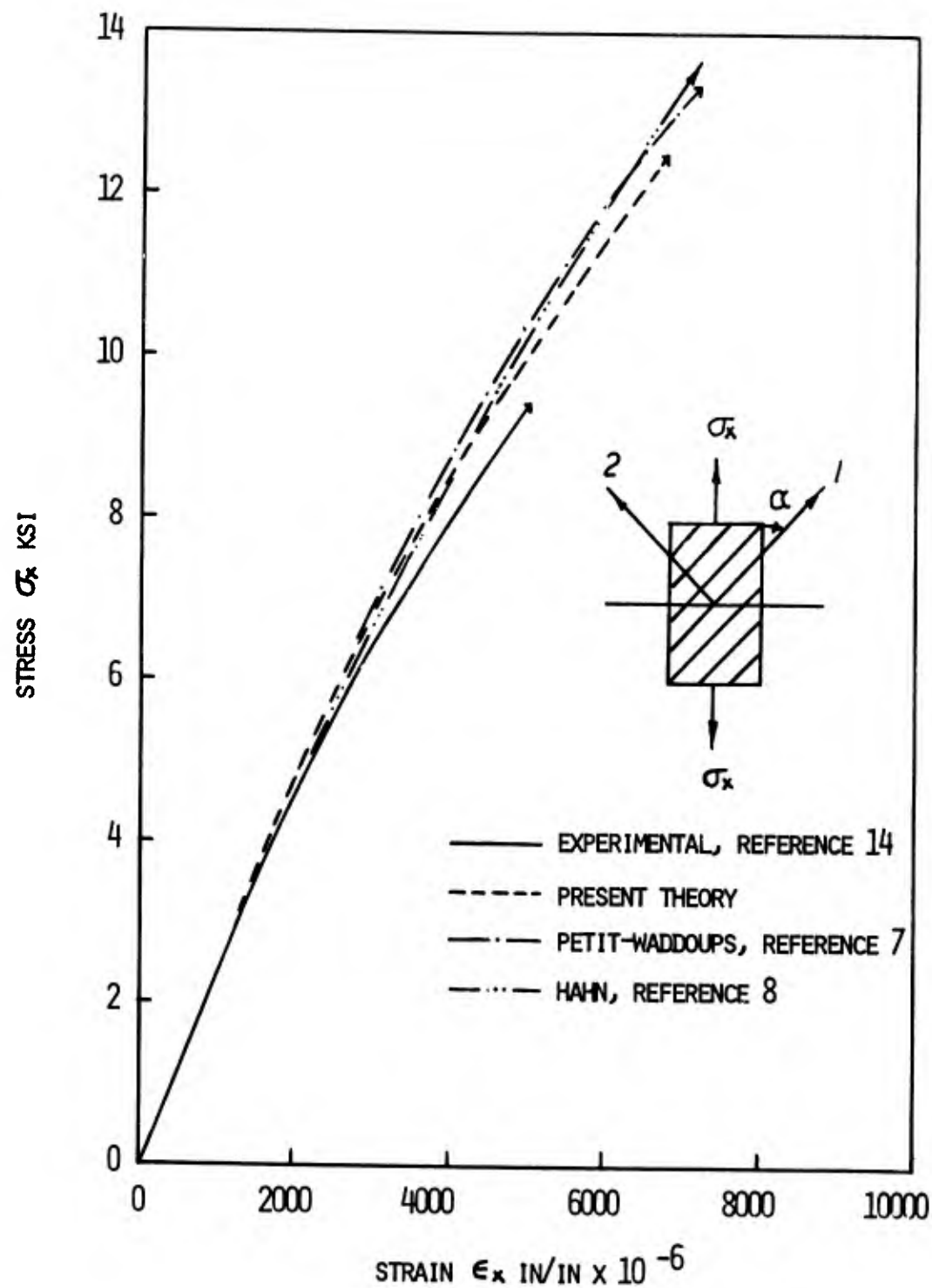


Figure 9. Boron-Epoxy 60° Off-Axis Coupon

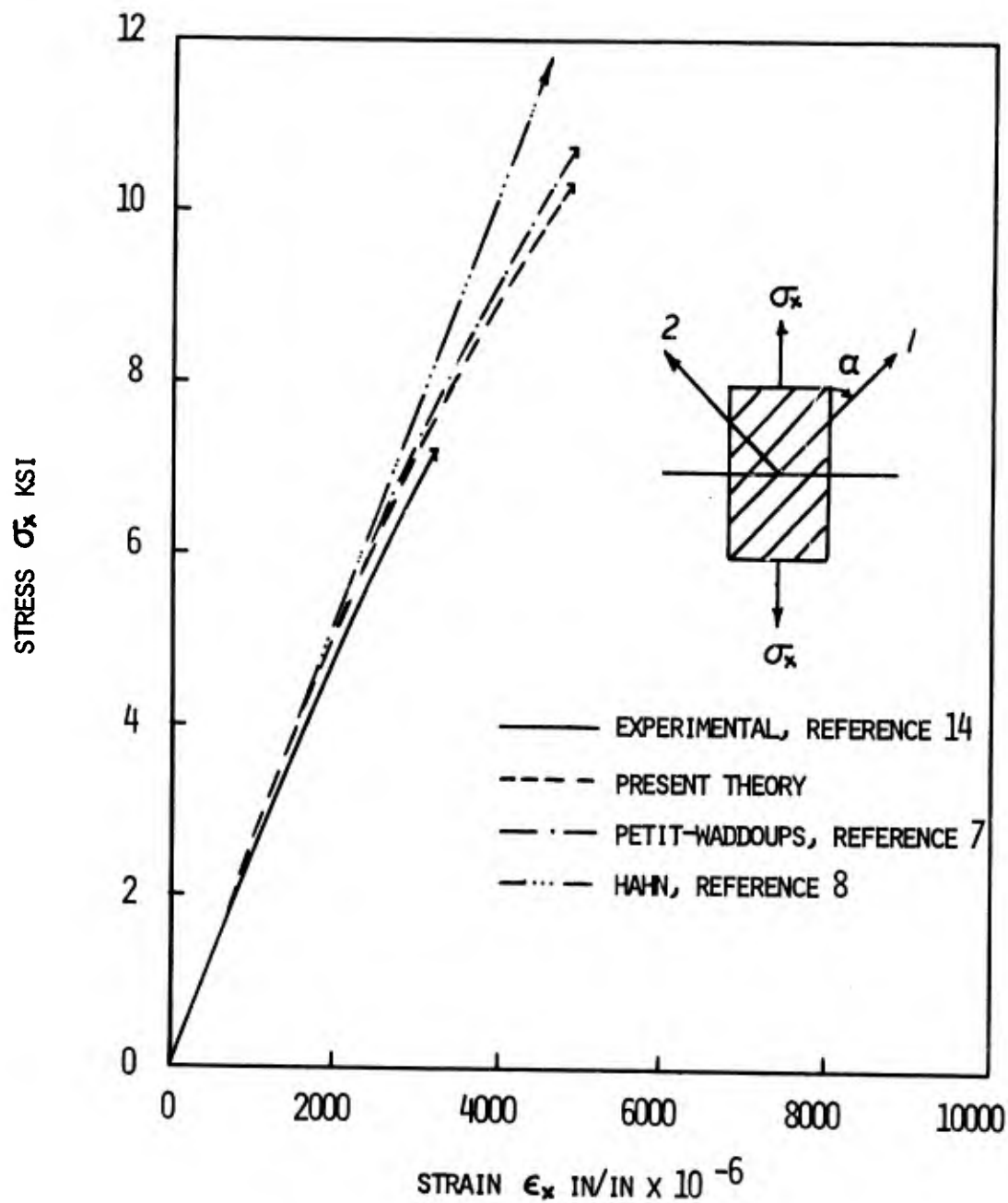


Figure 10. Boron-Epoxy 75° Off-Axis Coupon

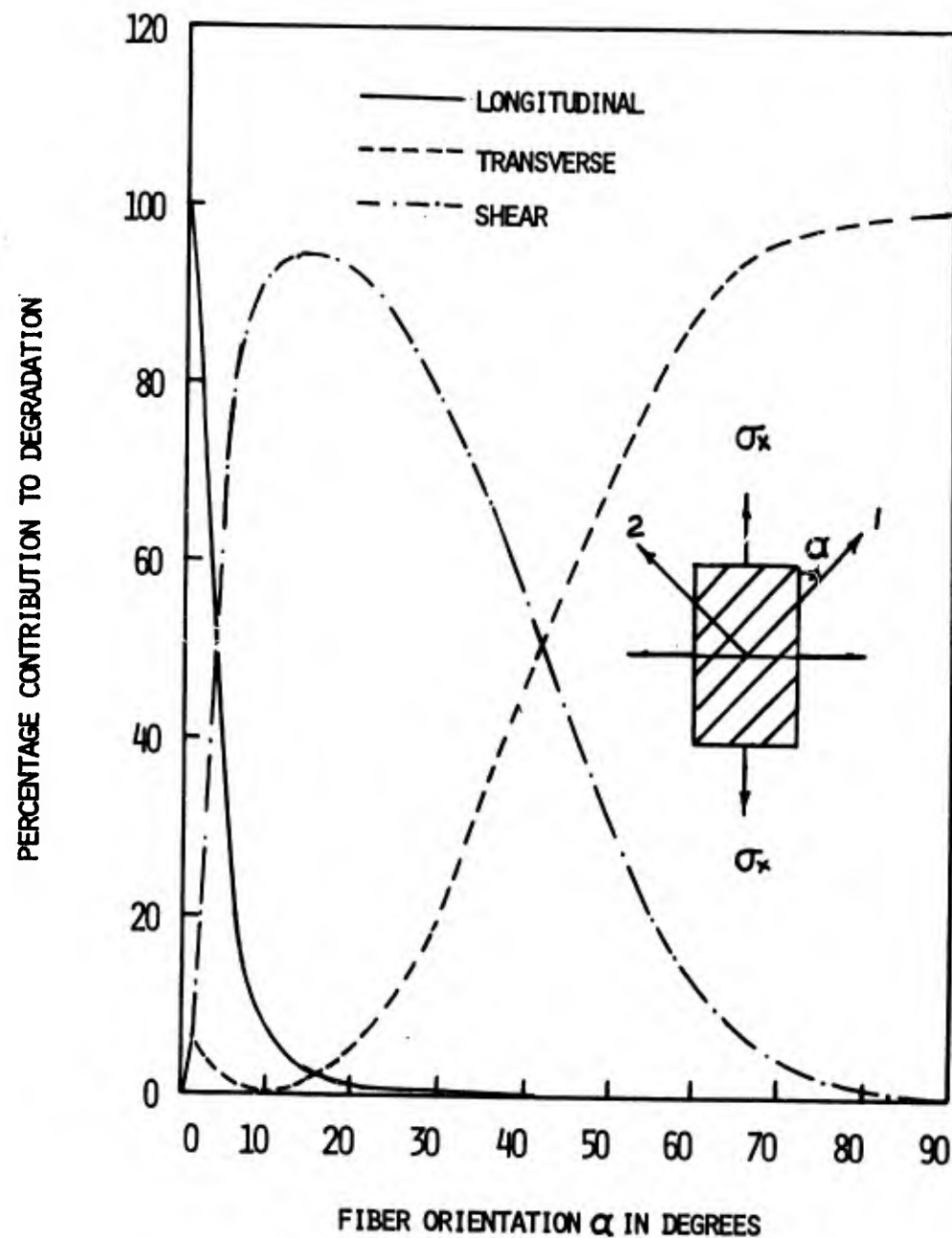


Figure 11. Percentage Contribution to Degradation of Off-Axis Specimens

TABLE I
STRENGTH AND DEGRADATION OF OFF-AXIS COUPONS

α	Failure Stresses ksi	Percentage Degradation (Eq. 31)		
		Longitudinal	Transverse	Shear
0°	190.50	100	0.	0.
2°	169.74	77.21	7.29	15.5
5°	104.50	27.59	1.05	71.36
10°	55.66	7.22	0.3	92.48
15°	38.31	3.18	2.68	94.14
30°	21.29	0.53	19.77	79.70
45°	16.04	0.11	57.83	42.06
60°	12.47	0.01	87.97	12.02
75°	10.39	0.01	98.12	1.87
90°	9.75	0.	100.	0.

On this basis, we would expect that for $\alpha = 10^\circ$ to 90° , failure planes would be parallel to the fiber orientations and failures would correspond to matrix failure modes. Figure 12 (References 14 and 15) appears to confirm this finding.

3. ANGLE PLY ($\pm\alpha^\circ$) LAMINATES

These laminates are fabricated from unidirectional laminas. To relate their analytical behavior to the basic experimental response of laminas, we used Equations 26 and 31. Theoretical failure stresses and contribution to degradation of 0° , $\pm 15^\circ$, $\pm 30^\circ$, $\pm 45^\circ$, and $(0^\circ/90^\circ)$ laminates subjected to various stress ratios are summarized in Tables II and III. To validate these results would require an experimental corroboration; relevant experimental data is almost nonexistent. Reference 11 contains the results of tests conducted on $(\pm 30^\circ)$, $(\pm 45^\circ)$, and $(\pm 60^\circ)$ laminates under uniaxial loads. Some experimental data from biaxial tests on $(\pm 45^\circ)$ and $(0^\circ/90^\circ)$ laminates is reported in Reference 16. Analytical stress-strain relations of $(\pm 45^\circ)$, $(\pm 30^\circ)$, and $(\pm 60^\circ)$ laminates under uniaxial loads were obtained using the present theory and techniques of References 7 and 9. A comparison of experimental and the analytical stress-strain responses (Figures 13 to 15) indicates a better correlation with the present theory. Figure 16 indicates that

- (a) For $\alpha = 0^\circ$ to 30° , longitudinal contribution to degradation decreases, shear and transverse contributions to degradation increase (transverse stresses being compressive).
- (b) For $\alpha = 30^\circ$ to 45° , longitudinal contribution to failure continues to decrease, shear contribution continues upward, and transverse contribution decreases.
- (c) For $\alpha = 45^\circ$, shear contribution reaches a maximum of 97.57% with longitudinal and transverse contributions being 0.71% and 1.72%.
- (d) For $\alpha = 45^\circ$ to 60° , shear contribution drops and transverse contribution rises sharply. Transverse contribution is due to tensile stresses.
- (e) For $\alpha = 60^\circ$ to 90° , the failure is essentially a transverse failure mode.



Figure 12. Failed Off-Axis Coupons

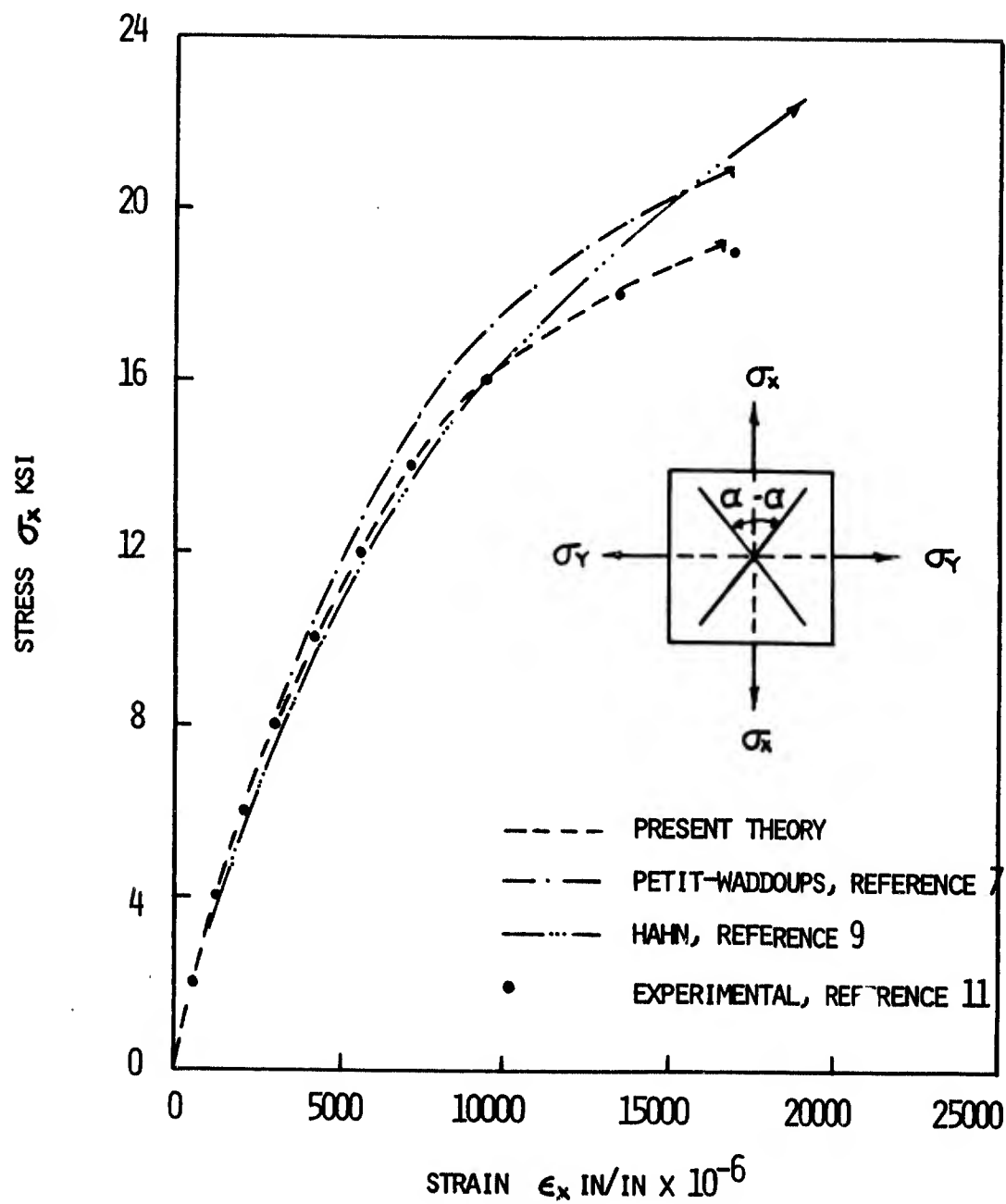
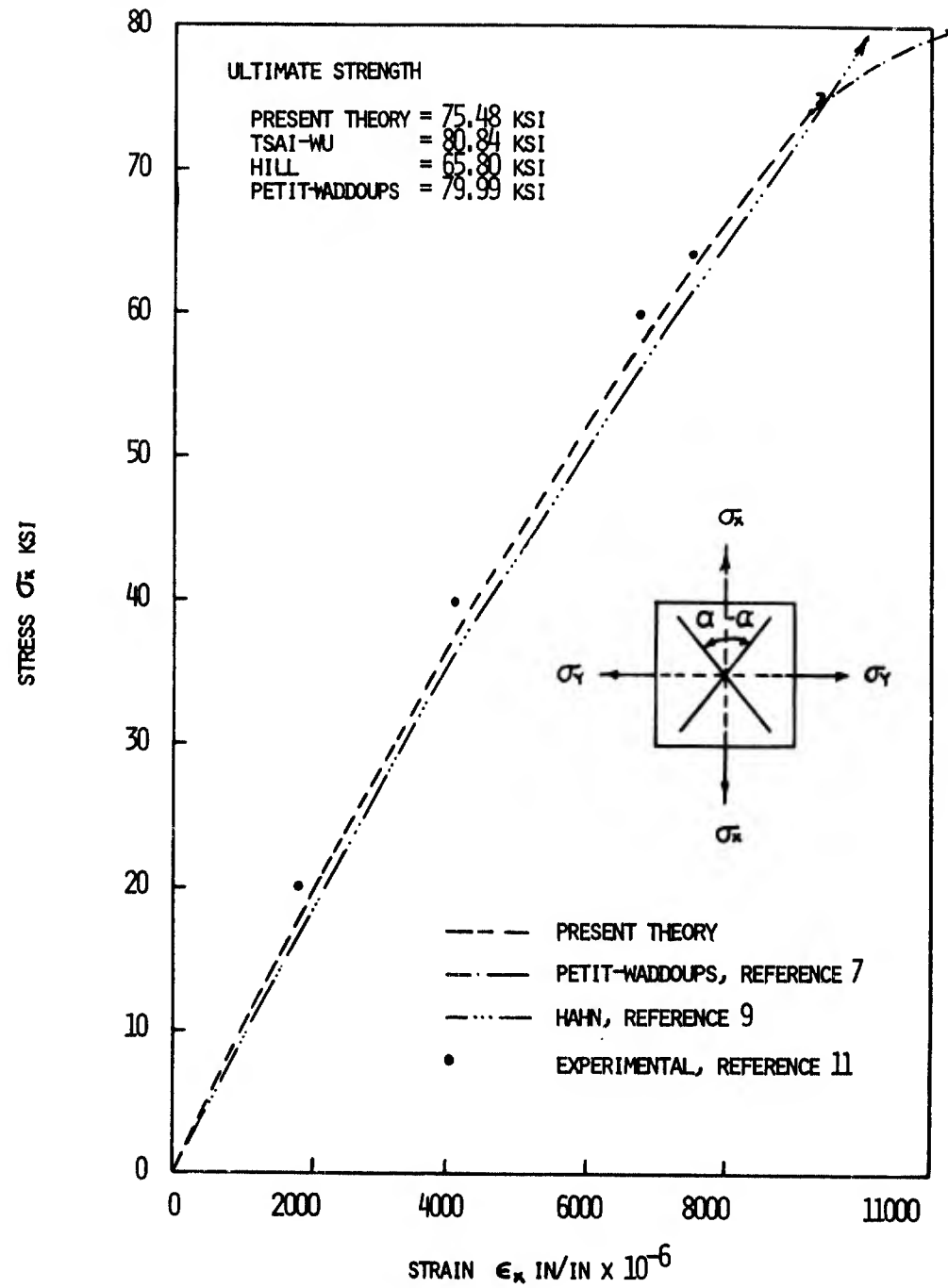


Figure 13. Response of $(\pm 45^\circ)$ Laminate Subjected to Stress σ_x Only

Figure 14. Response of ($\pm 30^\circ$) Laminate Subjected to Stress σ_x Only

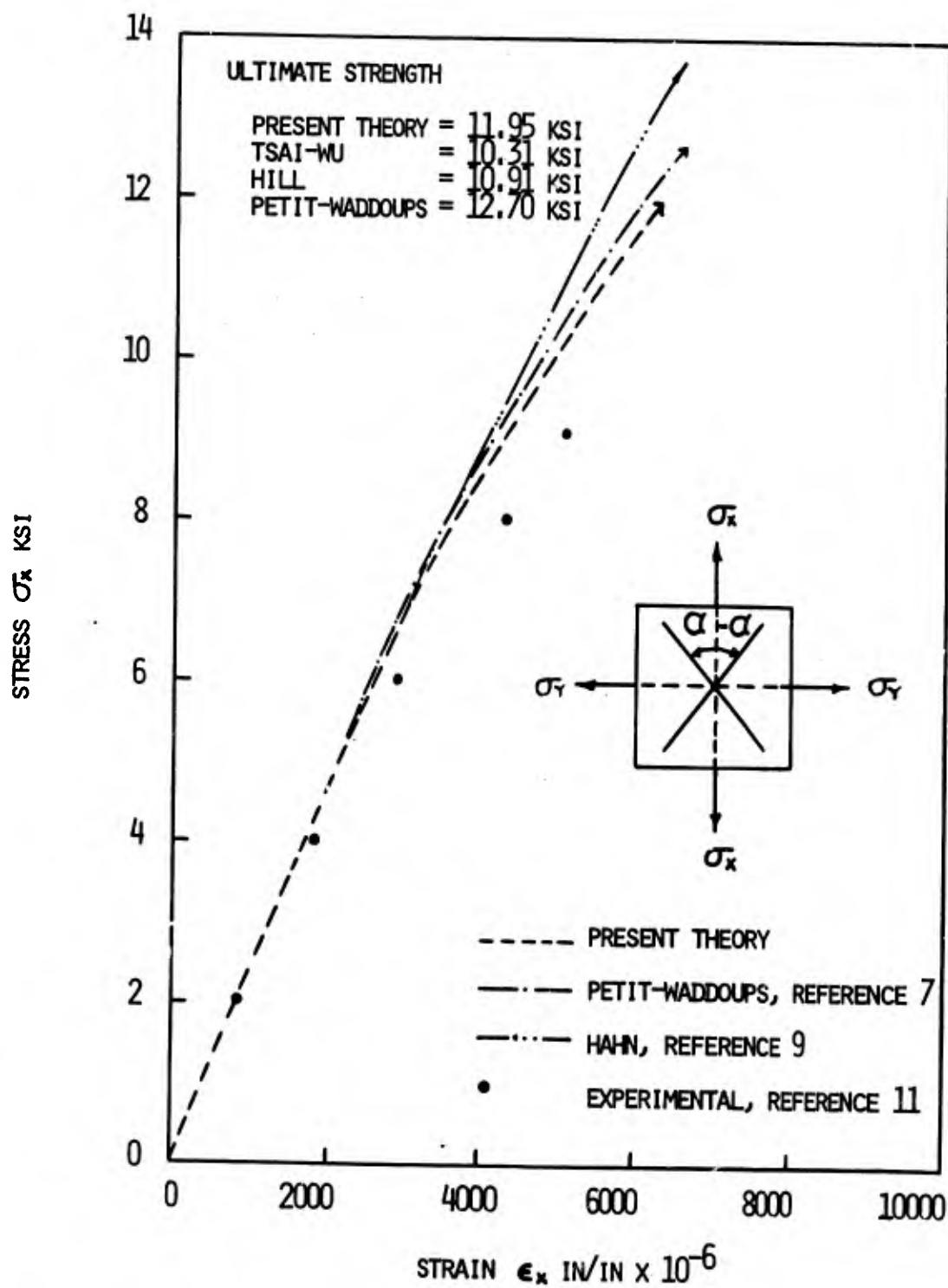


Figure 15. Response of ($\pm 60^\circ$) Laminate Subjected to Stress σ_x Only

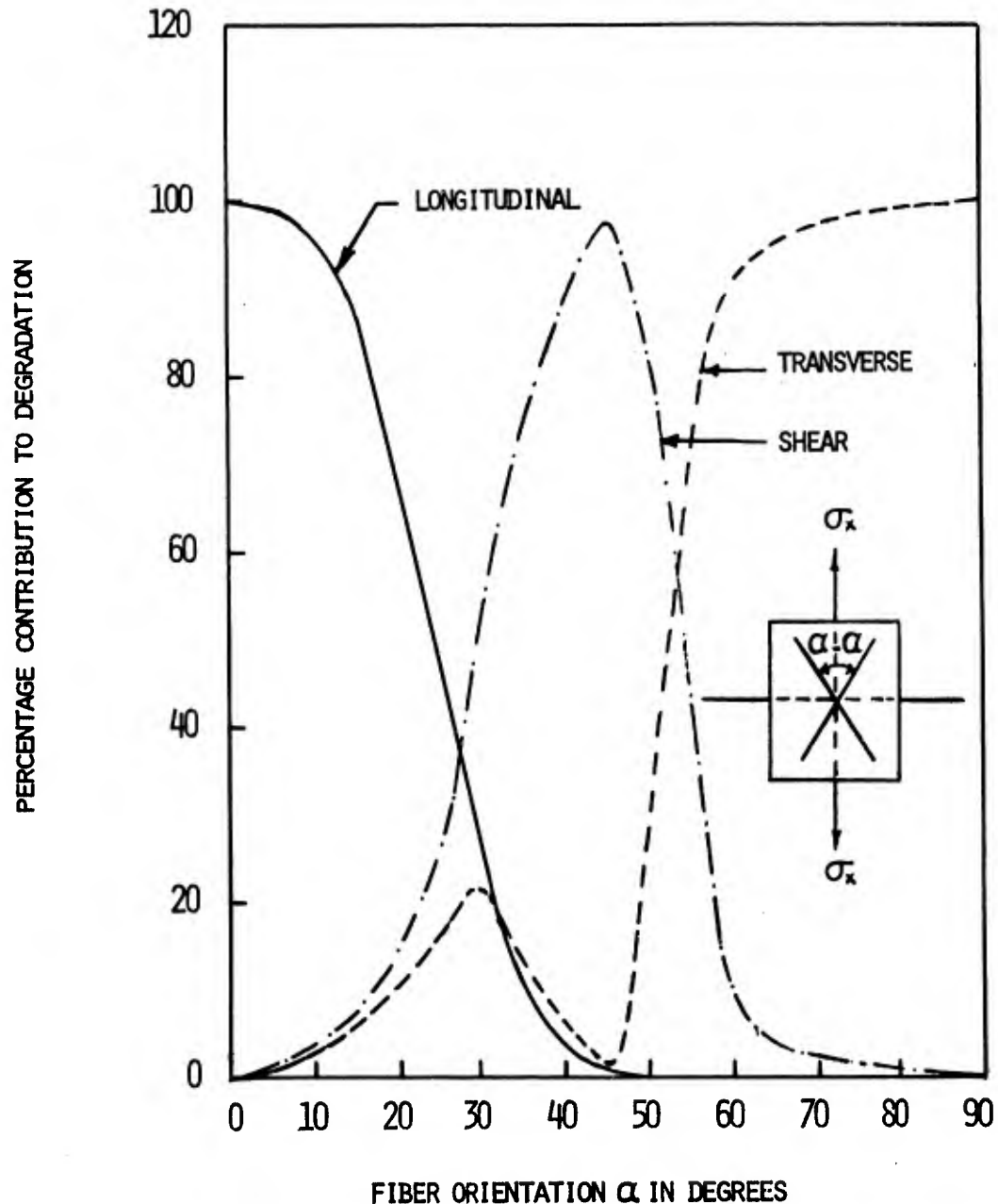


Figure 16. Percentage Contribution to Degradation of $(\pm\alpha^\circ)$ Laminates Subjected to Stress σ_x Only

Experimental stress-strain plots for ($\pm 45^\circ$) laminates subjected to biaxial loading are not available, so no comparison is possible. A comparison of theoretical and experimental strengths, however, for ($\pm 45^\circ$) laminates under biaxial loads is shown in Figure 17. The results do not agree too well with experimental data.

Lacking sufficient and reliable experimental data, full corroboration of the analytical technique of Sections II and III as applied to angle ply laminates is not feasible. However, some insight into their behavior may be obtained from the analytical results summarized in Tables II and III. Some of these results are shown in Figure 18. Figure 18 shows that transverse strength tends to increase with increasing angle α and longitudinal strength declines. For a given stress ratio, the points of maximum strength correspond to peaks of longitudinal contribution to degradation. In other regions either transverse or shear contribution to degradation dominates.

4. CROSS PLY ($0^\circ/90^\circ$) LAMINATES

A special case of angle ply laminates is ($0^\circ/90^\circ$) laminate with equal number of 0° and 90° plies. Its behavior is different from that of other laminates discussed so far. In unidirectional and angle ply laminates, there is only one failure state, but in ($0^\circ/90^\circ$) laminate, such a state occurs only for $\sigma_x/\sigma_y = 1:1$. For other stress ratios, σ_x/σ_y , transverse degradation of 0° or 90° plies does not result in a general failure of the laminate. Thus ($0^\circ/90^\circ$) laminate has two failure states, the initial failure state and the final failure state. After impairment of transverse load carrying capacity of 0° or 90° plies, the affected plies tend to unload transversely. The manner in which the unloading takes place is debatable. In the analysis reported herein, it is assumed that a transverse or shear impairment (i.e., on the occurrence of the matrix failure mode) the ply or plies affected by such impairment unload and transfer transverse and shear loads to the unaffected plies. This process of load transfer is assumed to continue till a general failure of the laminate occurs.

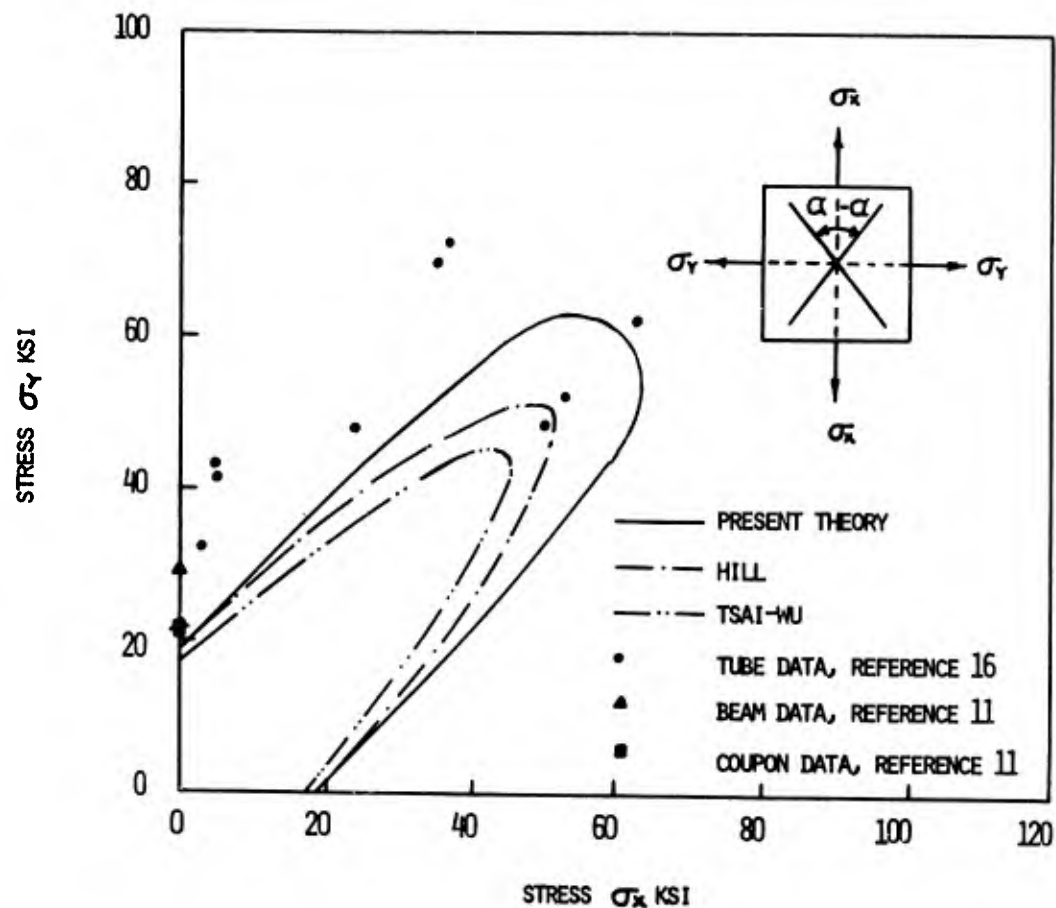


Figure 17. Strength Envelope for $(\pm 45^\circ)$ Laminate

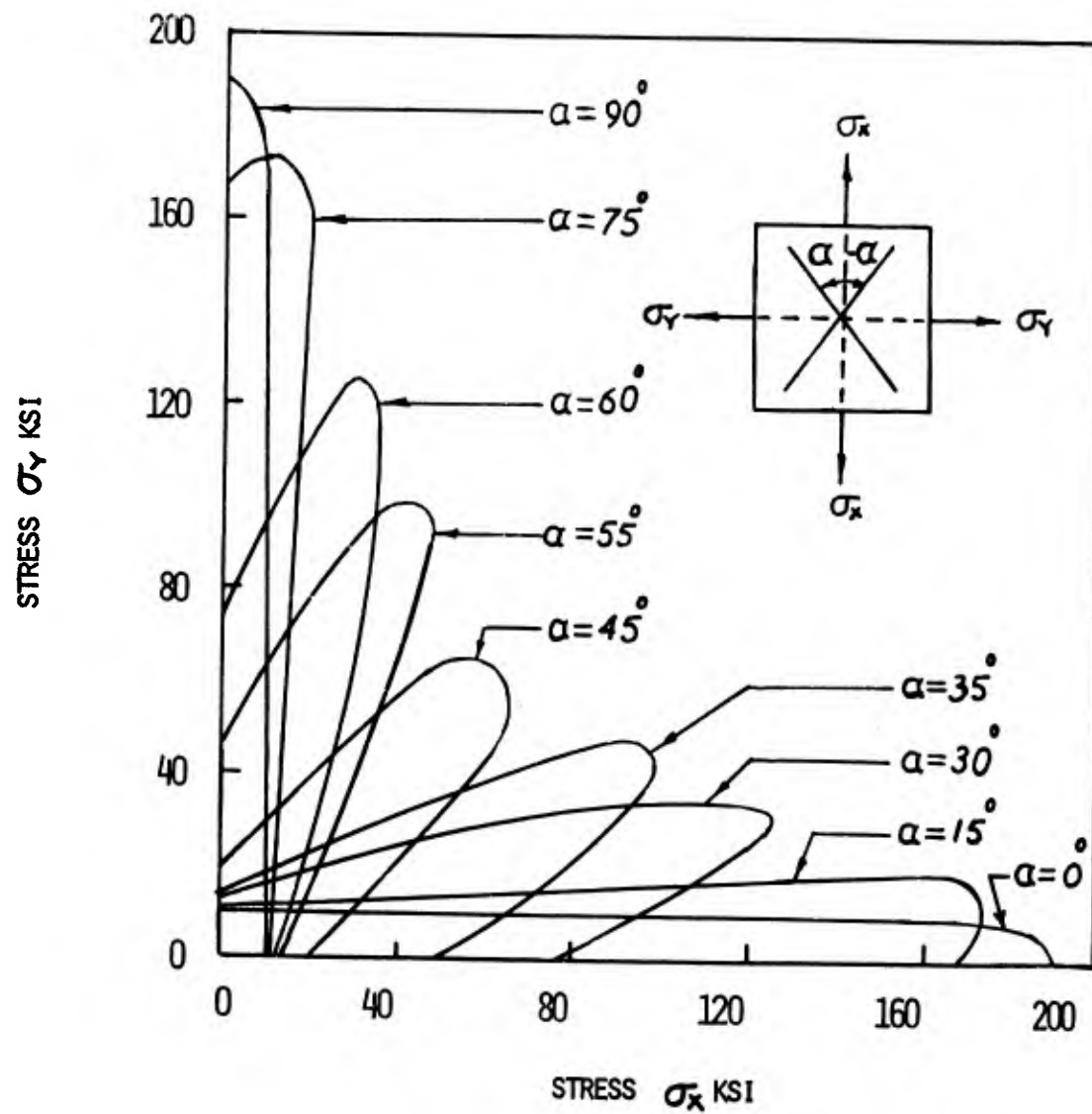


Figure 18. Strength Envelopes for (±α°) Laminates

TABLE II
FAILURE STRESSES FOR ($\pm\alpha^{\circ}$) AND ($0^{\circ}/90^{\circ}$) LAMINATES

No.	Stress Ratio: $\sigma_x \sigma_y \tau_{xy}$			Failure Stresses in ksi		$(0^{\circ}/90^{\circ})_c$
	0°	$\pm 15^{\circ}$	$\pm 30^{\circ}$	$\pm 45^{\circ}$		
1	0 1 0	0. :9.75:0.	0. :10.38:0.	0. :11.95:0.	0. :18.83:0.	0. :95.23:0.
2	1 4 0	2.44:9.77:0.	2.66:10.63:0.	3.25:12.99:0.	6.31:25.24:0.	22.96:91.31:0.
3	1 2 0	4.88:9.77:0.	5.42:10.84:0.	7.16:14.31:0.	18.40:36.80:0.	40.72:81.44:0.
4	3 4 0	7.32:9.77:0.	8.26:11.01:0.	11.75:15.66:0.	45.0 :60.0 :0.	51.93:69.24:0.
5	1 1 0	9.77:9.77:0.	11.19:11.19:0.	17.54:17.54:0.	60.63:60.63:0.	60.63:60.63:0.
6	4 3 0	12.99:9.74:0.	15.18:11.38:0.	26.70:20.02:0.	60.0 :45.0 :0.	69.24:51.93:0.
7	2 1 0	19.44:9.72:0.	22.99:11.49:0.	55.0 :27.50:0.	36.80:18.40:0.	81.44:40.72:0.
8	4 1 0	38.98:9.72:0.	54.10:13.53:0	127.45:31.86:0.	25.24: 6.31:0.	91.31:22.96:0.
9	1 0 0	190.5 :0. :0.	166.23:0. :0.	75.48:0. :0.	18.83: 0. :0.	95.23: 0. :0.

TABLE III
DEGRADATION OF ($\pm 60^\circ$) AND ($0^\circ/90^\circ$) LAMINATES

No.	Stress Ratio σ_x σ_y τ_{xy}	PERCENT DEGRADATION												0°			90°		
		0°			$\pm 15^\circ$			$\pm 30^\circ$			$\pm 45^\circ$			0°			90°		
L	T	S	L	T	S	L	T	S	L	T	S	L	T	S	L	T	S		
1	0 1 0	0.	100.0	0.	0.007	98.67	1.32	0.	90.73	9.27	0.71	1.72	97.57	0.00	99.97	0.	99.27	0.001	0.
2	1 4 0	0.004	99.28	0.	0.003	98.72	1.27	0.06	91.16	8.79	2.00	4.85	93.15	3.64	87.95	0.	91.18	8.82	0.
3	1 2 0	0.021	98.59	0.	0.04	98.18	1.21	0.24	91.55	8.21	6.00	14.38	79.62	13.06	74.52	0.	69.41	30.59	0.
4	3 4 0	0.072	97.90	0.	0.13	97.26	1.14	0.62	91.85	7.52	21.31	48.84	29.85	22.32	68.28	0.	49.09	50.91	0.
5	1 1 0	0.154	97.20	0.	0.27	96.39	1.07	1.35	91.98	6.67	30.78	69.22	0.	30.78	69.22	0.	30.78	69.22	0.
6	4 3 0	0.311	96.25	0.	0.54	95.30	0.99	3.14	89.56	5.15	21.31	48.84	29.85	49.09	50.91	0.0	22.32	68.28	0.
7	2 1 0	0.785	96.47	0.	1.36	92.90	0.82	12.98	79.88	1.46	6.00	14.38	79.62	69.41	30.59	0.	13.06	74.52	0.
8	4 1 0	3.533	88.98	0.0	8.08	83.85	0.32	71.34	1.65	27.01	2.00	4.85	93.15	91.18	8.82	0.	3.64	87.95	0.
9	1 0 0	100.0	0.	0.	86.74	6.32	6.94	27.50	21.47	51.03	0.71	1.72	97.57	99.27	0.001	0.	0.	99.97	0.

L = Longitudinal

T = Transverse

S = Shear

On the basis of the above assumption, the analytical strength envelope contributions to degradation for various stress ratios and stress-strain curves were obtained (Figure 19 to 24) and compared with the available experimental data (Reference 16). In addition analytical stress-strain curves were obtained using the technique of Reference 7. Though the analytical-experimental correlation appears to be reasonable, there are some features of the experimental data which need to be kept in mind in evaluating this correlation. These features are the differences in the properties of materials used in the experimental and analytical programs, preload effects, and the reported experimental strain data. The strains reported are the readings of the three elements of the 45° strain gage rosette and not the components of strain. Hence no quantitative comparison is feasible.

5. $(0^\circ/\pm\alpha^\circ)_s$ LAMINATES

In this category, only $(0^\circ/\pm60^\circ)_s$ and $(0^\circ/\pm45^\circ)_s$ laminates were studied. Stresses and contributions to degradation at failure for these laminates are given in Tables IV and V. Values for the $(0^\circ/\pm60^\circ)_s$ laminate are plotted in Figures 25 and 26. We observed that

- (a) For $\sigma_y/\sigma_x < 1$, transverse degradation of 0° plies causes initial failure, but the laminate is still capable of carrying additional load;
- (b) For $\sigma_x/\sigma_y = 1$, all plies fail simultaneously, resulting in the general failure of the laminate;
- (c) For $\sigma_x/\sigma_y > 1$, transverse degradation of $\pm60^\circ$ plies causes initial failure, which is followed by a general failure when 0° plies degrade.

No biaxial data is available to substantiate the analytical results. A comparison of experimental results obtained from testing coupons of $(0^\circ/\pm60^\circ)_s$ laminate under uniaxial loading with the theoretical results is shown in Figures 27 and 28; the correlation is very good for the stress ratio $\sigma_x/\sigma_y = 1:0$, but it is far from acceptable for the stress ratio $\sigma_x/\sigma_y = 0:1$.

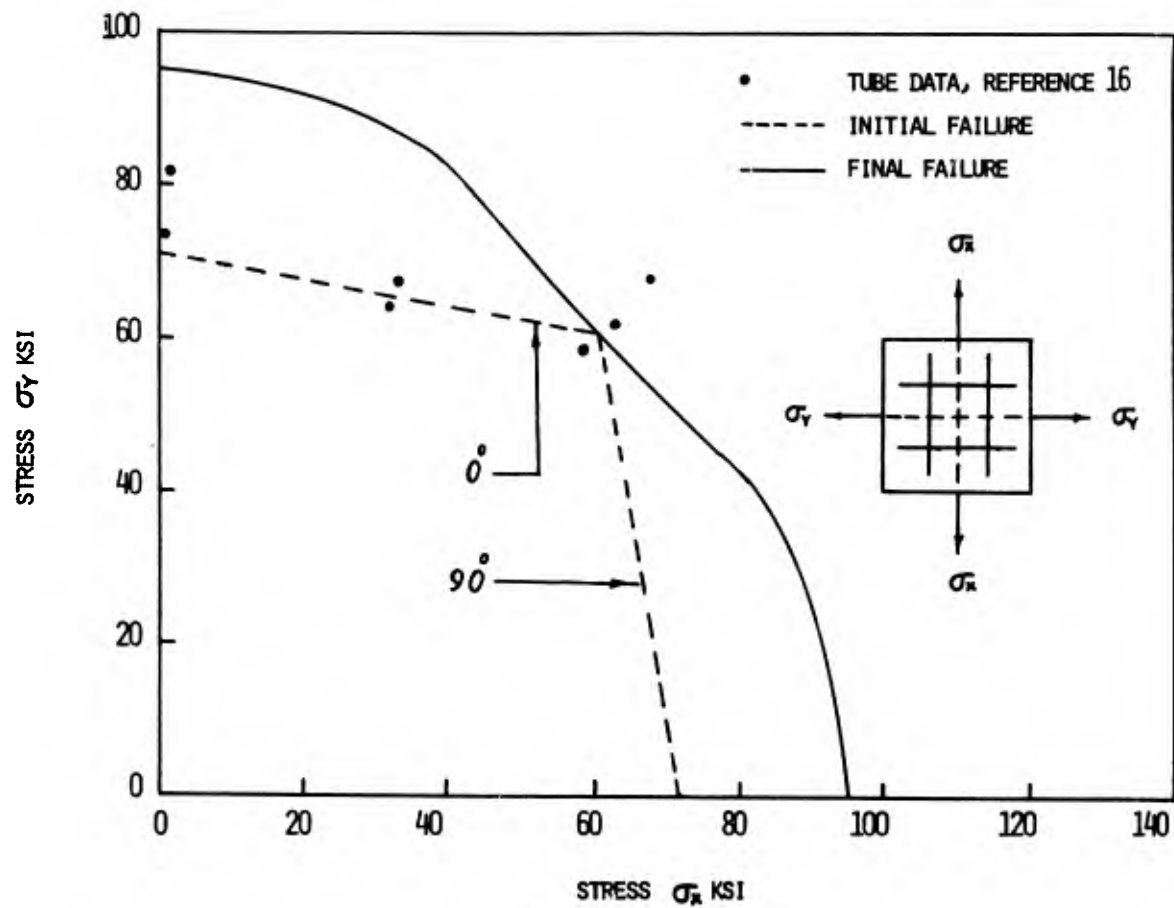


Figure 19. Strength Envelope for $(0^\circ/90^\circ)$ Laminate

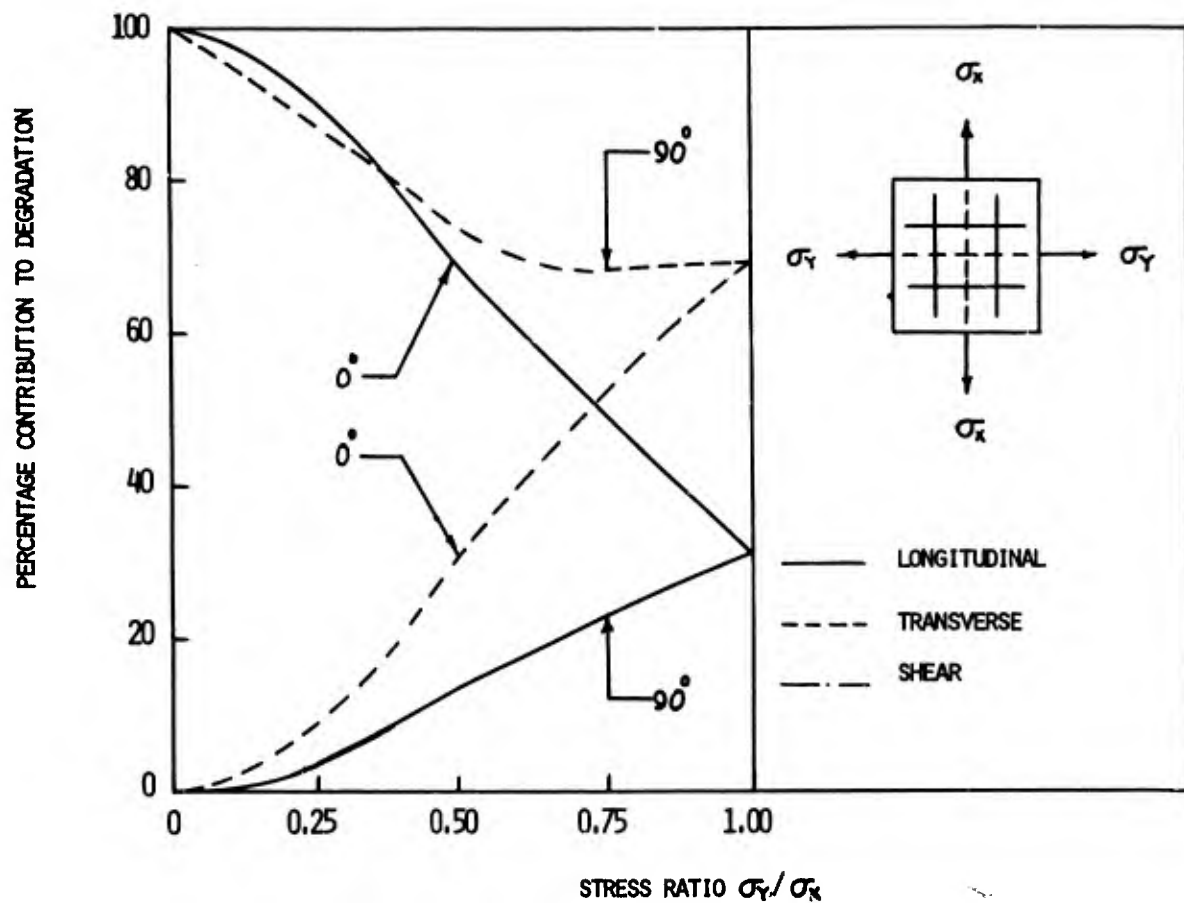


Figure 20. Percentage Contribution to Degradation of $(0^\circ/90^\circ)$ Laminate Subjected to Various Stress Ratios

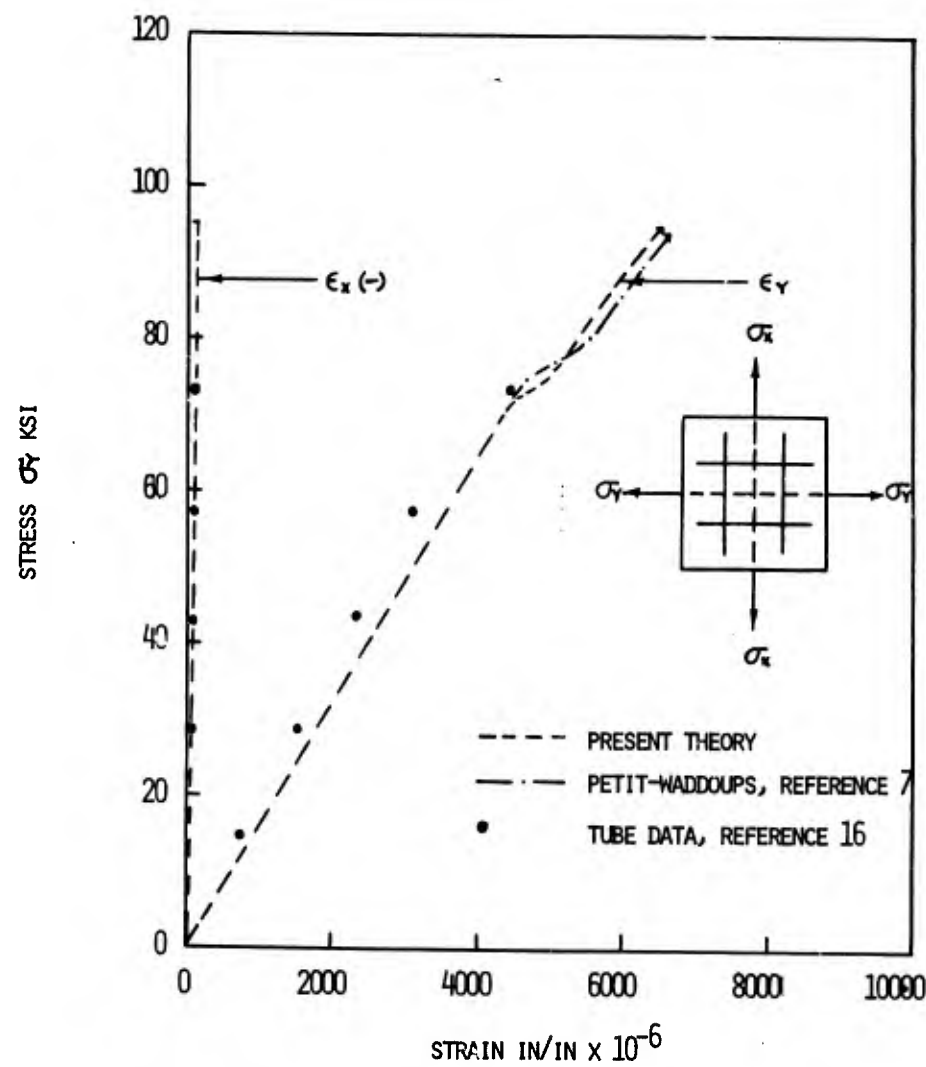


Figure 21. Stress-Strain Response of $(0^\circ/90^\circ)$ Laminate Subjected to a Stress Ratio, $\sigma_x/\sigma_y = 0:1$

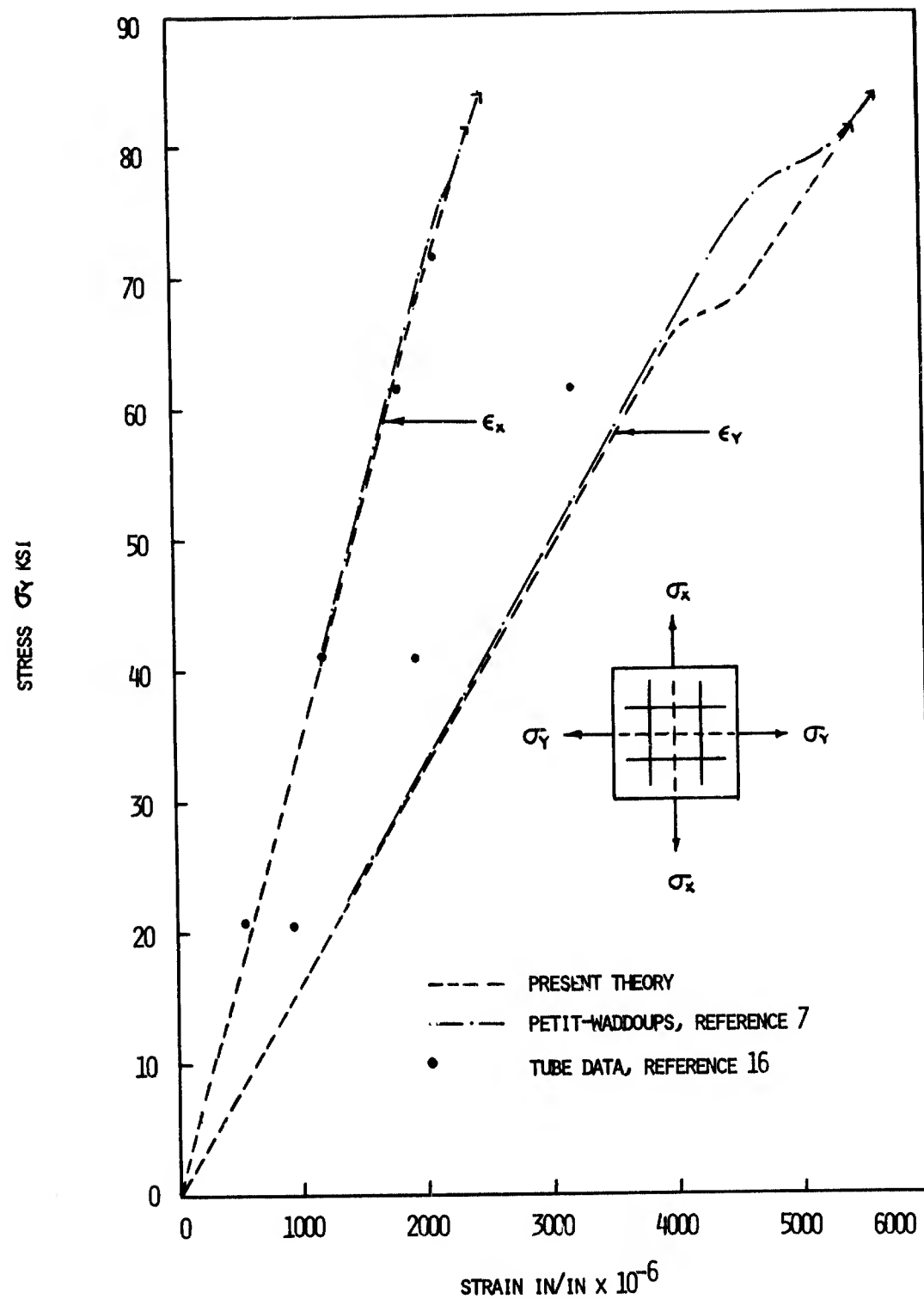


Figure 22. Stress-Strain Response of $(0^\circ/90^\circ)$ Laminate Subjected to a Stress Ratio, $\sigma_x/\sigma_y = 1:2$

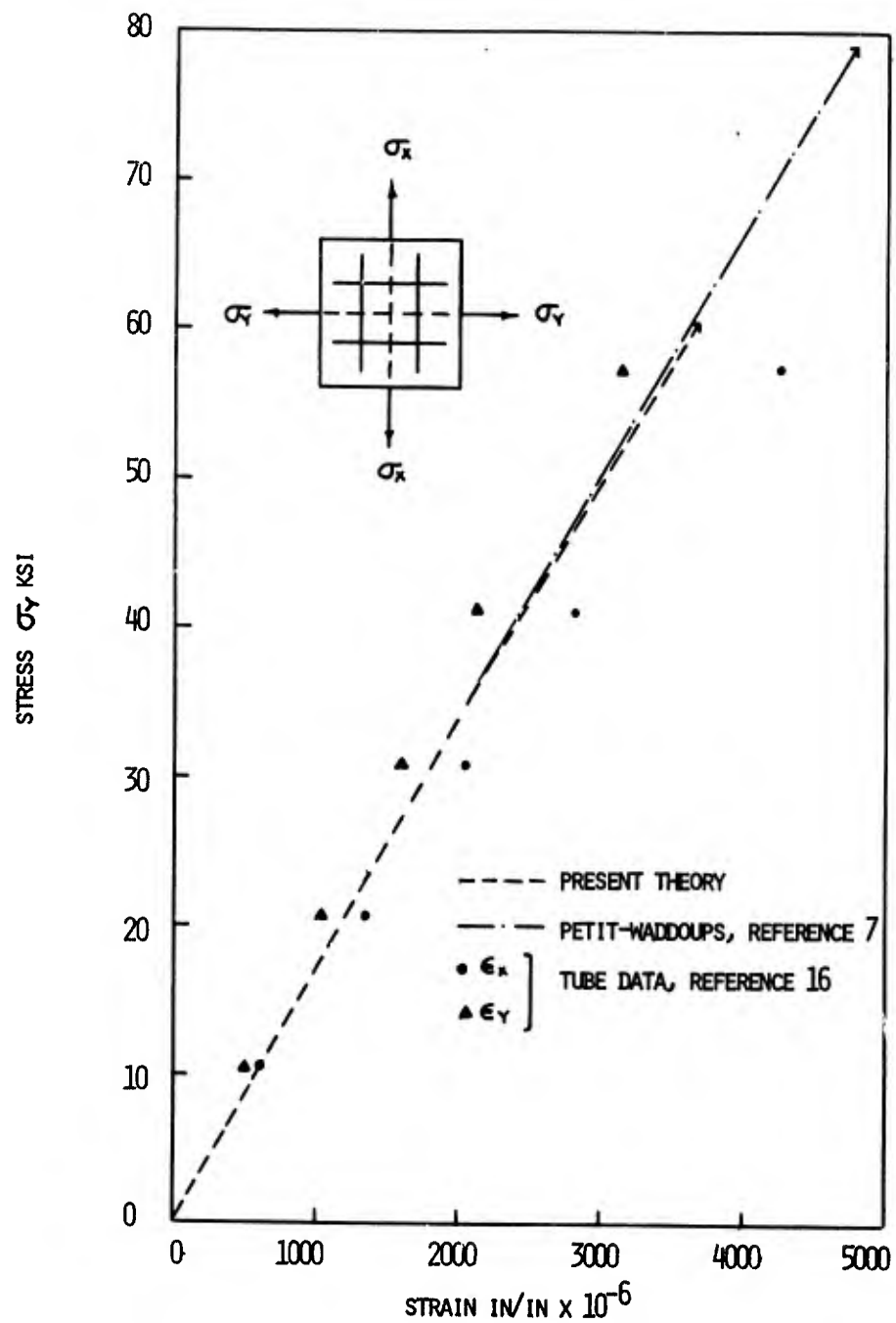


Figure 23. Stress-Strain Response of (0°/90°) Laminate
Subjected to a Stress Ratio, $\sigma_x/\sigma_y = 1:1$

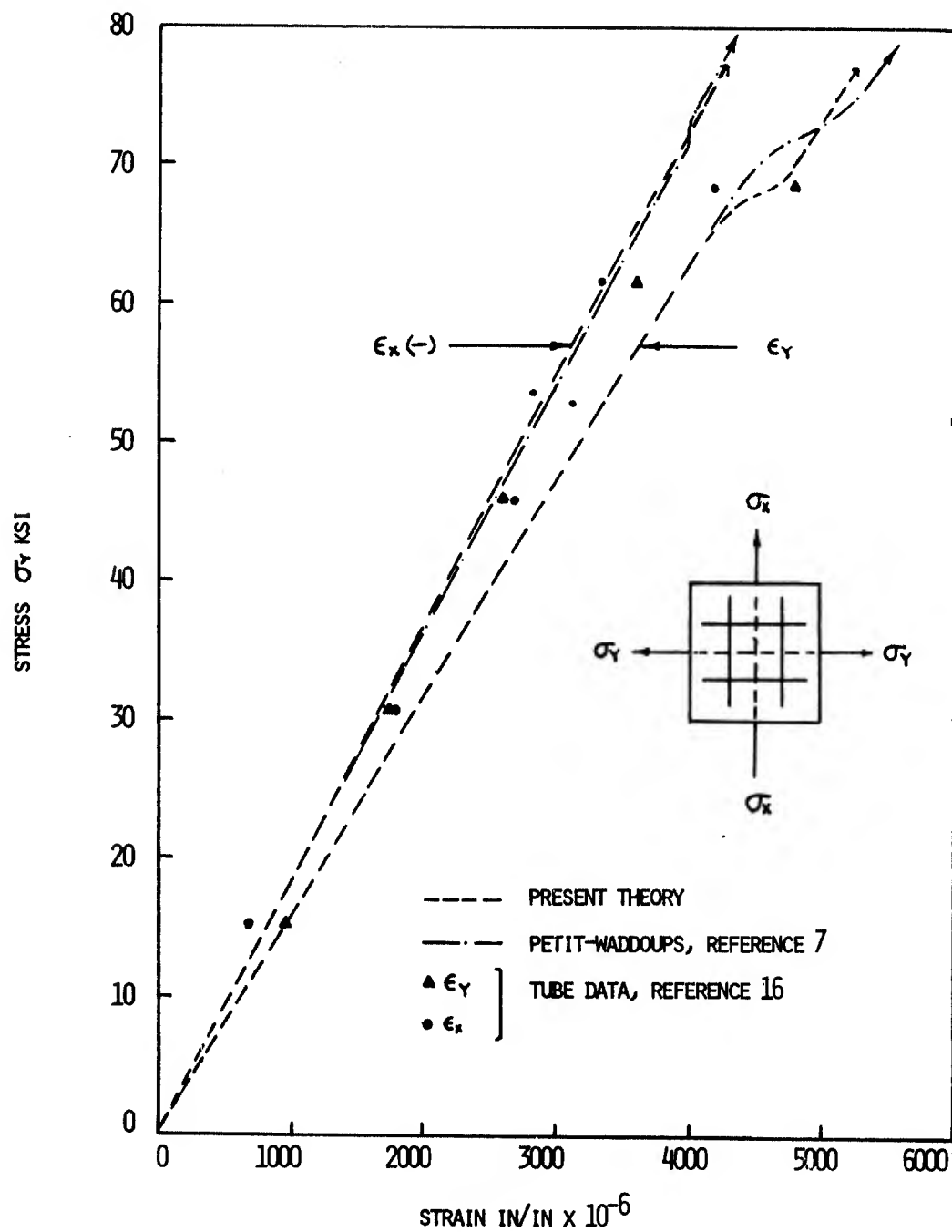


Figure 24. Stress-Strain Response of $(0^\circ/90^\circ)$ Laminate
Subjected to a Stress Ratio, $\sigma_x/\sigma_y = -1:1$

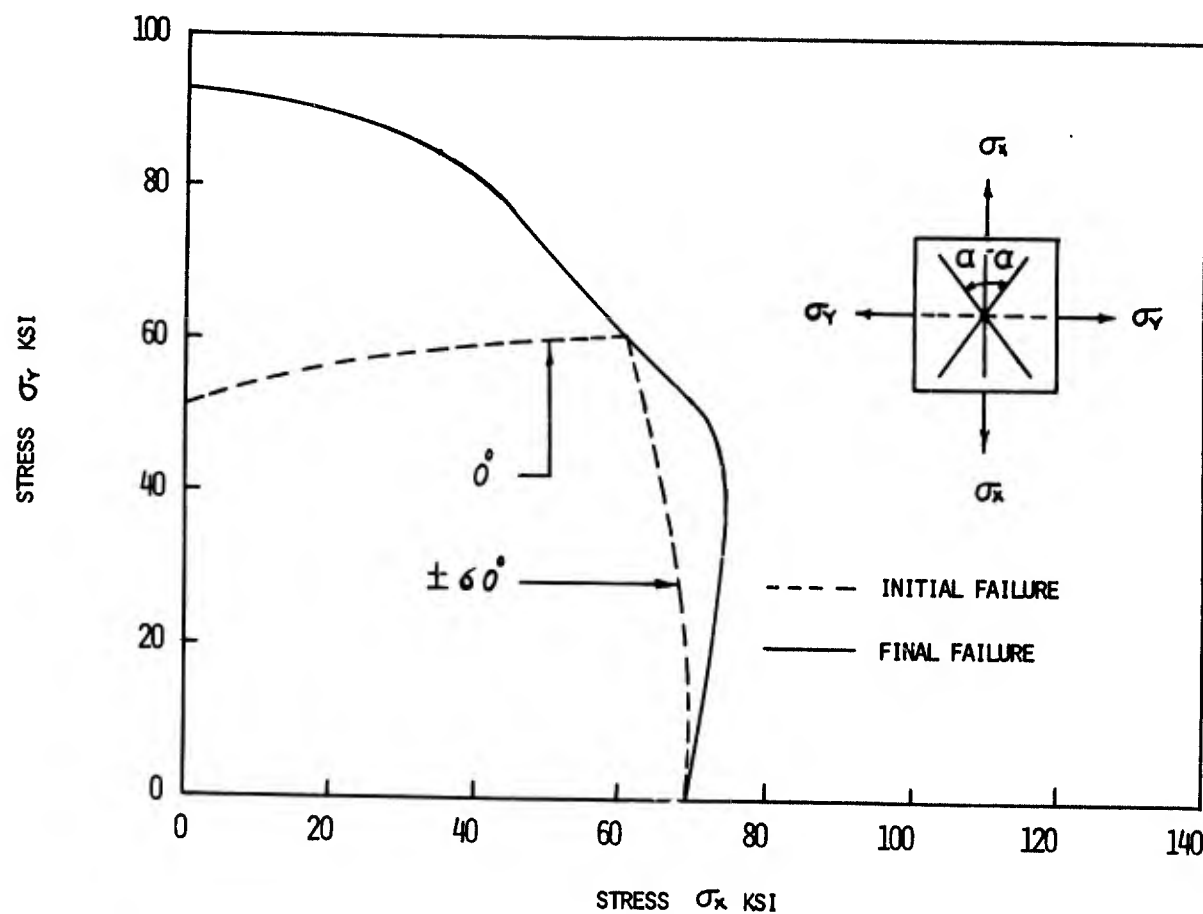


Figure 25. Strength Envelope for $(0^\circ/\pm 60^\circ)_s$ Laminate

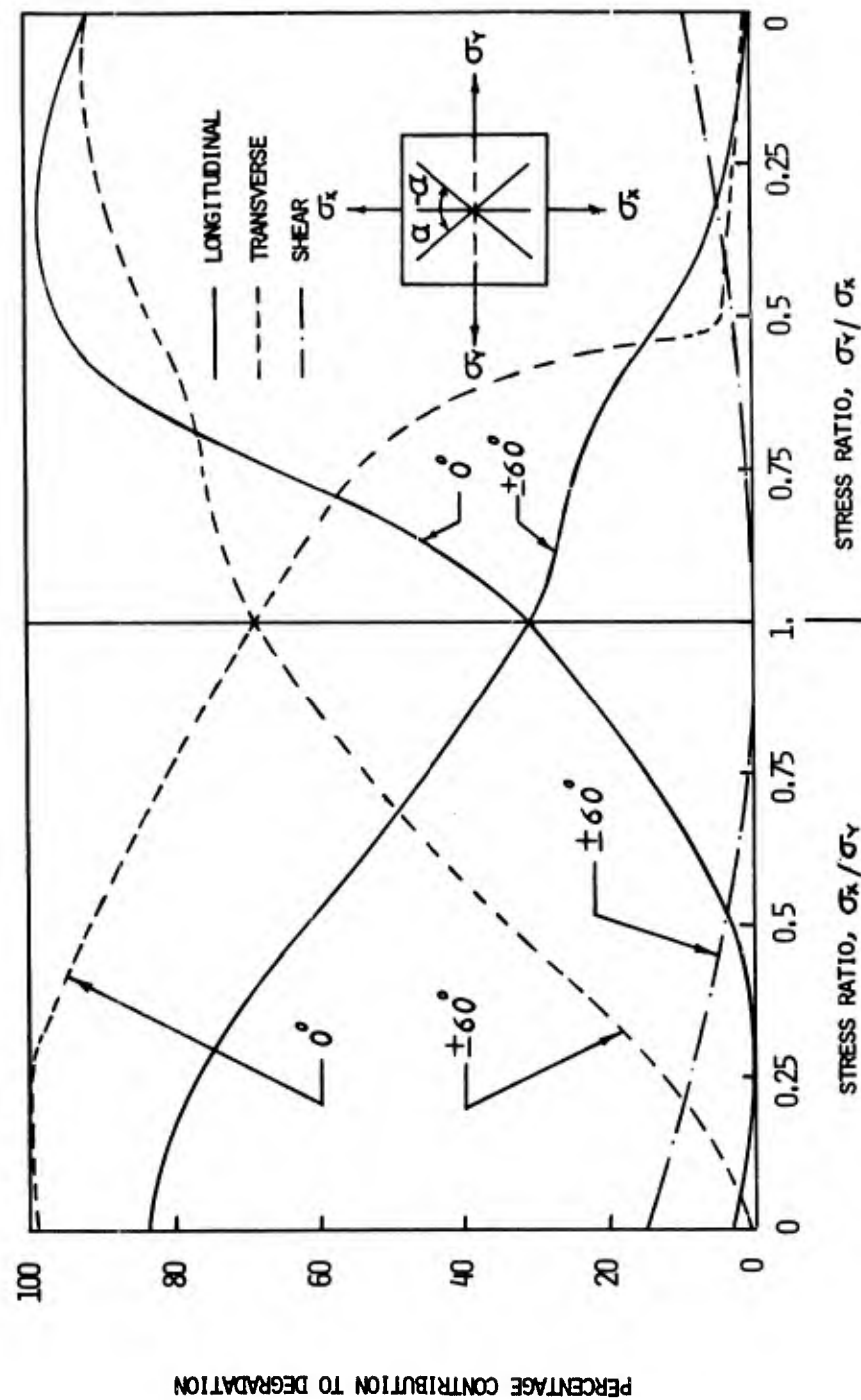


Figure 26. Percentage Contribution to Degradation of $(0^\circ/\pm 60^\circ)_s$ Laminate Subjected to Various Stress Ratios

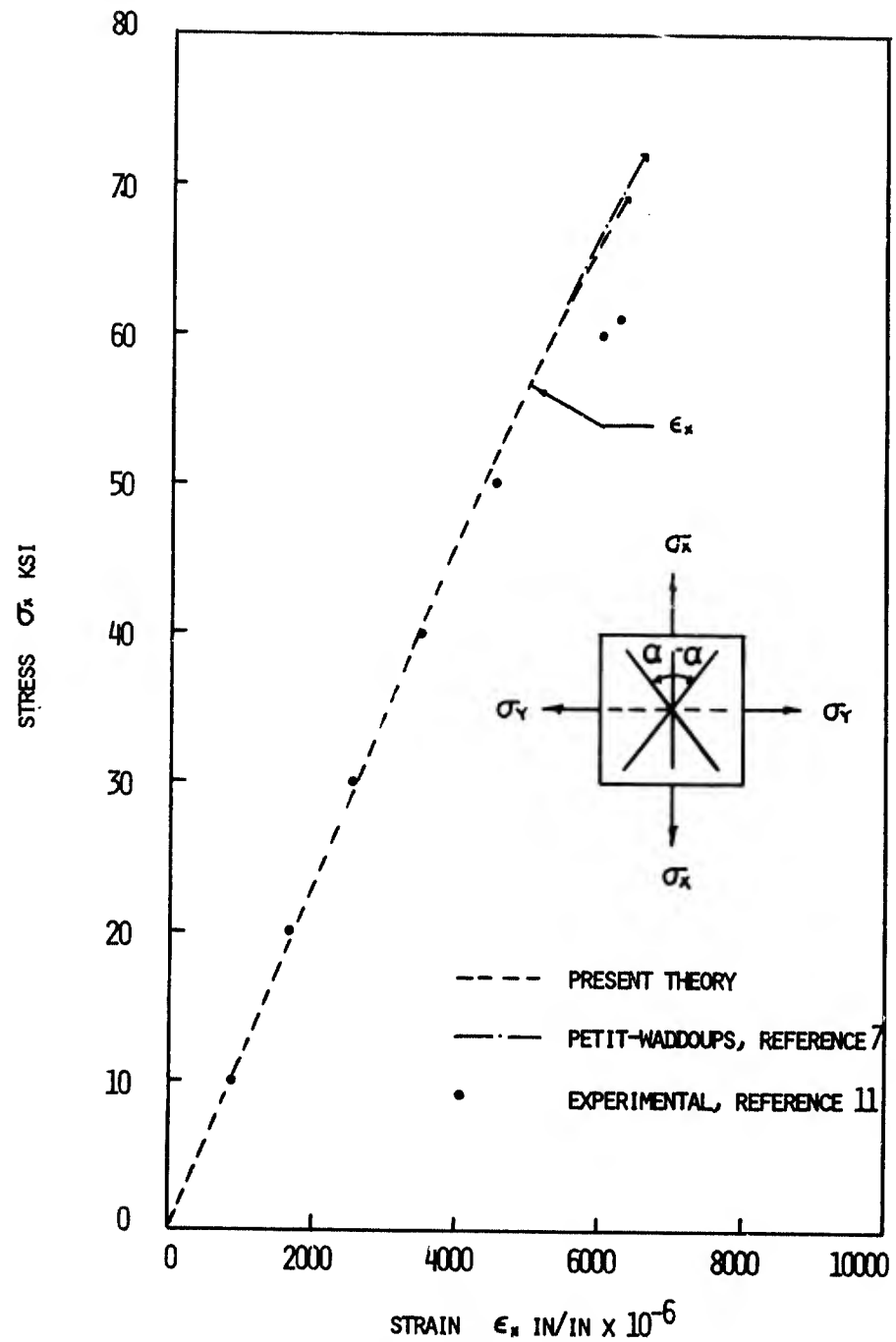


Figure 27. Stress-Strain Response of $(0^\circ/\pm 60^\circ)_s$ Laminate
Subjected to Stress σ_x only

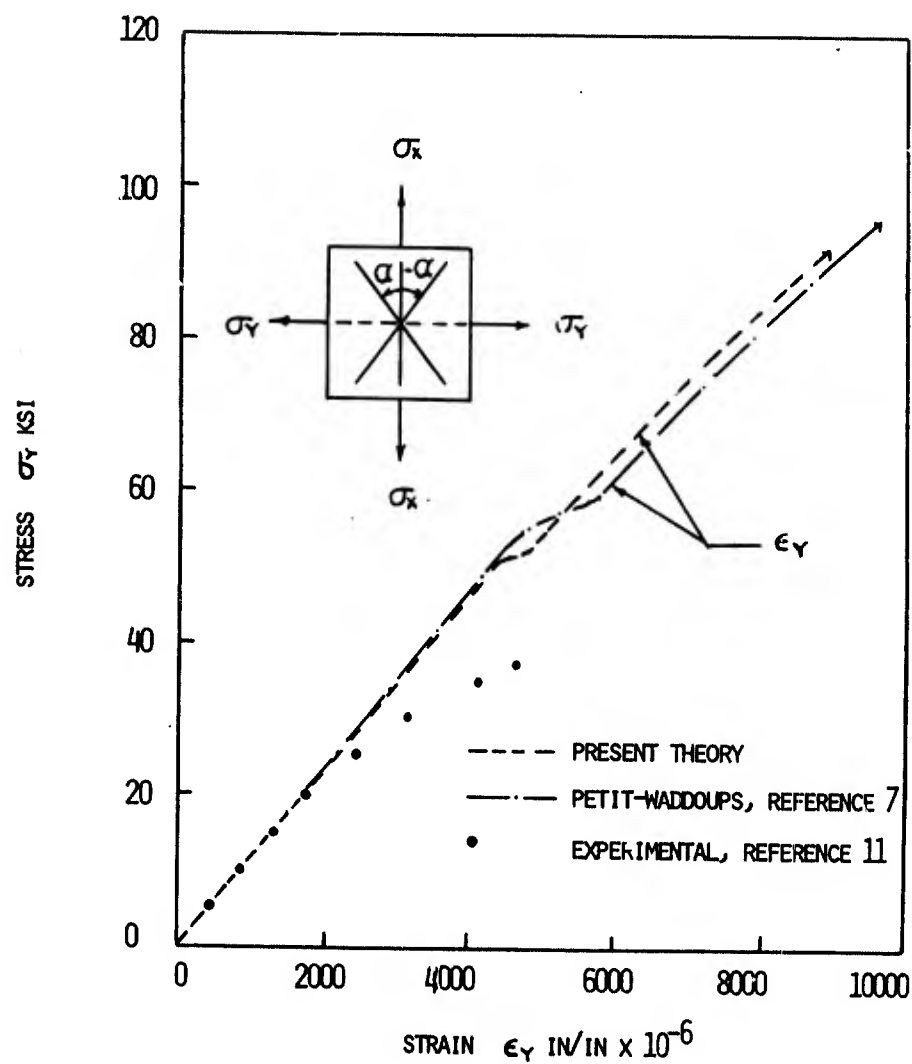


Figure 28. Stress-Strain Response of $(0^\circ/\pm 60^\circ)_s$ Laminate
Subjected to Stress σ_y only

Figures 29 and 30 show the analytical strength envelope and contribution to degradation of $(0/\pm 45^\circ)_s$ laminate subjected to various stress ratios. Since no experimental data is available, we can make no comparison.

6. MULTIDIRECTIONAL LAMINATES

Innumerable multidirectional laminates can be fabricated from unidirectional plies. For this study, we considered only $(0^\circ/\pm 45^\circ/90^\circ)$ family laminates. There are three laminates in this category, namely $(0^\circ/\pm 45^\circ/90^\circ)_s$, $(0^\circ_2/\pm 45^\circ/90^\circ)_s$, and $(0^\circ/\pm 45^\circ/0^\circ/90^\circ)_s$, for which some experimental data is available for comparison with the analytical results. Failure stresses and contributions to degradation for the above three laminates are summarized in Tables VI to VIII.

Figures 31 to 36 show the strength envelope, contributions to degradation, and stress-strain curves for the $(0^\circ/\pm 45^\circ/90^\circ)_s$ laminate. The strength envelope is symmetric about the stress ratio of 1:1. The agreement between predicted and experimentally determined strengths for the stress ratios σ_y/σ_x of 1:0 and 2:1 is very close (Figure 31). For the stress ratio σ_x/σ_y of 1:1 there is general agreement but the experimental values have considerable scatter. In this laminate, the initial failure is due to the transverse degradation of 0° plies for stress ratios $0 < \sigma_x/\sigma_y < 1$. The final failure is due to degradation of 90° plies for stress ratios of $0 < \sigma_x/\sigma_y < 1/2$ and by degradation of $\pm 45^\circ$ plies for stress ratios $\sigma_x/\sigma_y = 1/2$ to 1. For the stress ratio $\sigma_x/\sigma_y = 1:1$, all plies fail simultaneously; the qualitative correlation between analytical and experimental stress-strain curves was very good, as shown by Figures 33 to 36.

In the case of the $(0^\circ_2/\pm 45^\circ/90^\circ)_s$ laminate, no experimental stress-strain data is available. For this reason only failure stresses (experimental and analytical) are compared in Figure 37. The agreement between these is reasonable. The contributions to degradation of the laminate for various stress ratios are shown in Figure 38.

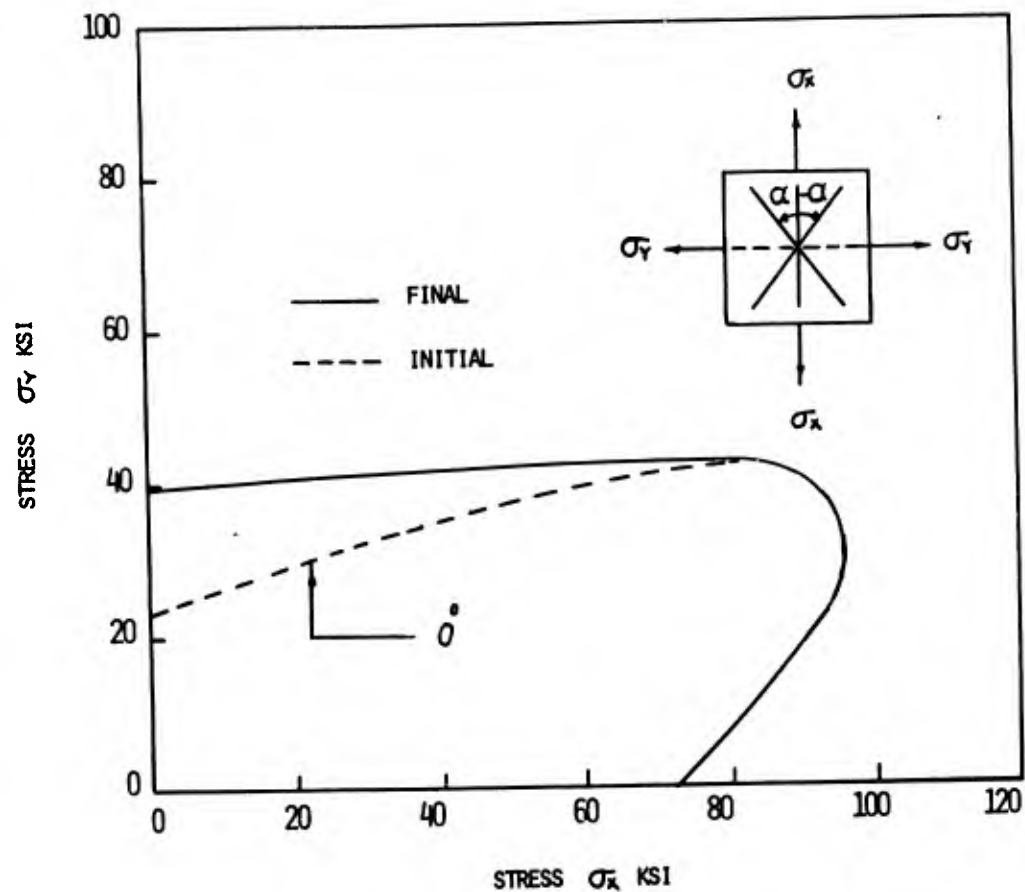


Figure 29. Strength Envelope for $(0^\circ/\pm 45^\circ)_s$ Laminate

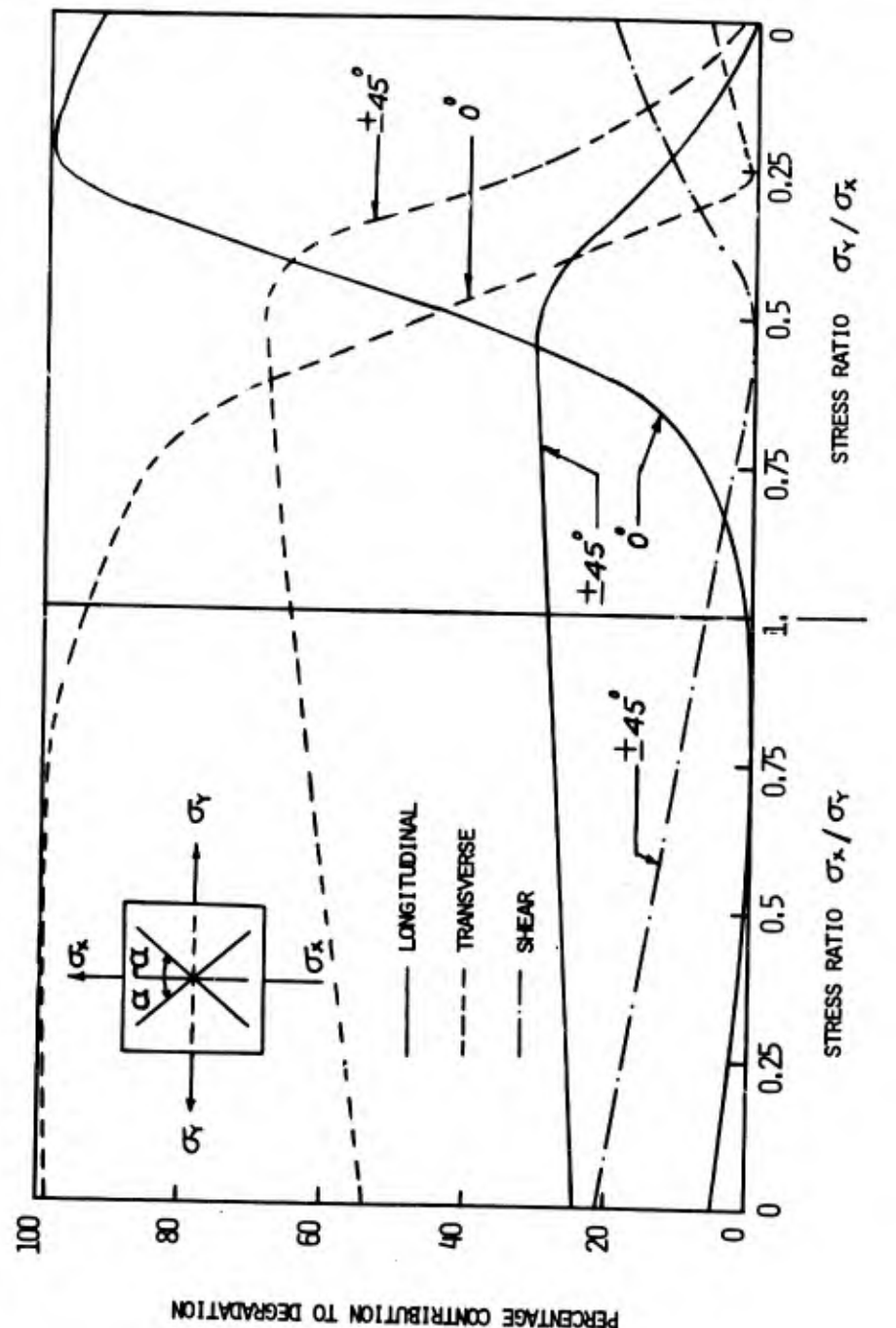


Figure 30. Percentage Contribution to Degradation of $(0^\circ/\pm 45^\circ)_s$ Laminate Subjected to Various Stress Ratios

TABLE IV
FAILURE STRESSES AND PERCENTAGE DEGRADATION FOR $(0^\circ/\pm 60^\circ)_s$ LAMINATES

No.	Stress Ratio	Stresses σ_{ki}			Initial Failure						Final Failure						Final Failure					
					Percentage Degradation			Stresses σ_{ki}			Percentage Degradation						Stresses σ_{ki}			Percentage Degradation		
		σ_x	σ_y	τ_{xy}	L	T	S	0° Pliés			$\pm 60^\circ$ Pliés			σ_x	σ_y	τ_{xy}	L	T	S	0° Pliés	$\pm 60^\circ$ Pliés	
1	0 1 0	0.	50.81	0.	1.00	99.0	0.	20.93	0.15	4.59	0.	92.31	0.	3.86	99.0	0.	83.86	0.70	15.44			
2	1 4 0	13.76	55.05	0.	0.06	99.88	0.	24.65	4.44	3.27	22.37	89.49	0.	0.25	99.88	0.	77.65	12.88	9.47			
3	1 2 0	28.70	57.40	0.	1.93	91.73	0.	26.97	16.92	1.65	40.36	80.72	0.	3.25	91.73	0.	61.80	34.18	4.02			
4	3 4 0	44.31	59.08	0.	11.72	80.80	0.	28.92	38.68	0.44	51.99	69.32	0.	15.28	80.80	0.	45.44	53.64	0.92			
5	1 1 0	60.40	60.40	0.	30.77	69.23	0.	30.77	69.23	0.	60.40	60.40	0.	30.77	69.23	0.	30.69	69.23	0.			
6	4 3 0	63.63	47.72	0.	42.67	32.06	0.	19.39	75.76	0.52	69.34	52.03	0	65.54	34.46	0.	24.06	75.75	0.52			
7	2 1 0	66.67	33.33	0.	57.52	6.34	0.	9.66	82.45	2.27	74.20	37.10	0.	95.44	4.56	0.	12.11	82.45	2.27			
8	4 1 0	69.41	17.35	0.	76.49	1.19	0.	2.77	90.10	5.42	72.02	18.00	0.	97.45	2.55	0.	2.93	90.10	5.42			
9	1 0 0	68.75	0.	0.	91.35	1.22	0.	0.01	90.86	9.13	68.75	0.	0.	91.35	1.22	0.	0.01	90.86	9.13			

L = Longitudinal

T = Transverse

S = Shear

TABLE V
FAILURE STRESSES AND PERCENTAGE DEGRADATION FOR $(0^\circ/\pm 45^\circ)_s$ LAMINATES

No	Stress Ratio	Stresses σ_{ai}			Initial Failure						Final Failure						0° Plies		
					Percentage Degradation			Stresses σ_{ai}			Percentage Degradation			0° Plies			$\pm 45^\circ$ Plies		
		σ_x	σ_y	τ_{xy}	σ_x	σ_y	τ_{xy}	L	T	S	L	T	S	σ_x	σ_y	τ_{xy}	L	T	S
1	0 1 0	0.	23.38	0.	1.09	98.91	0.	5.58	13.45	6.09	0.	39.85	0.	4.83	98.91	0.	24.10	54.50	21.40
2	1 4 0	6.35	25.39	0.	0.58	99.42	0.	7.02	16.82	5.43	10.10	40.40	0.	2.46	99.42	0.	25.11	57.24	17.65
3	1 2 0	13.85	27.70	0.	0.18	99.82	0.	8.89	21.17	4.69	20.59	41.16	0.	0.87	99.82	0.	26.37	59.92	13.71
4	3 4 0	22.66	30.21	0.	0.	99.60	0.	11.27	26.68	3.84	31.05	41.40	0.	0.09	99.60	0.	27.66	62.29	*10.05
5	1 1 0	32.81	32.81	0.	1.00	93.78	0.	14.20	33.32	2.59	41.81	41.81	C.	0.61	93.78	0.	28.65	64.74	6.61
6	4 3 0	49.24	36.93	0.	7.17	86.73	0.	19.64	45.38	1.06	55.66	41.74	0.	6.99	84.73	0.	29.91	67.40	2.69
7	2 1 0	84.69	42.34	0.	43.69	46.12	0.	30.73	68.96	0.31	86.69	42.34	0.	43.69	46.12	0.	30.73	68.96	0.31
8	4 1 0	94.10	23.52	0.	99.17	0.83	0.	13.96	32.77	11.54	94.10	23.52	0.	99.17	0.83	0.	13.96	32.77	11.54
9	1 0 0	72.40	0.	0.	92.68	7.32	0.	1.17	2.85	19.72	72.4	0.	0.	92.68	7.32	0.	1.17	2.85	19.72

L = Longitudinal
T = Transverse
S = Shear

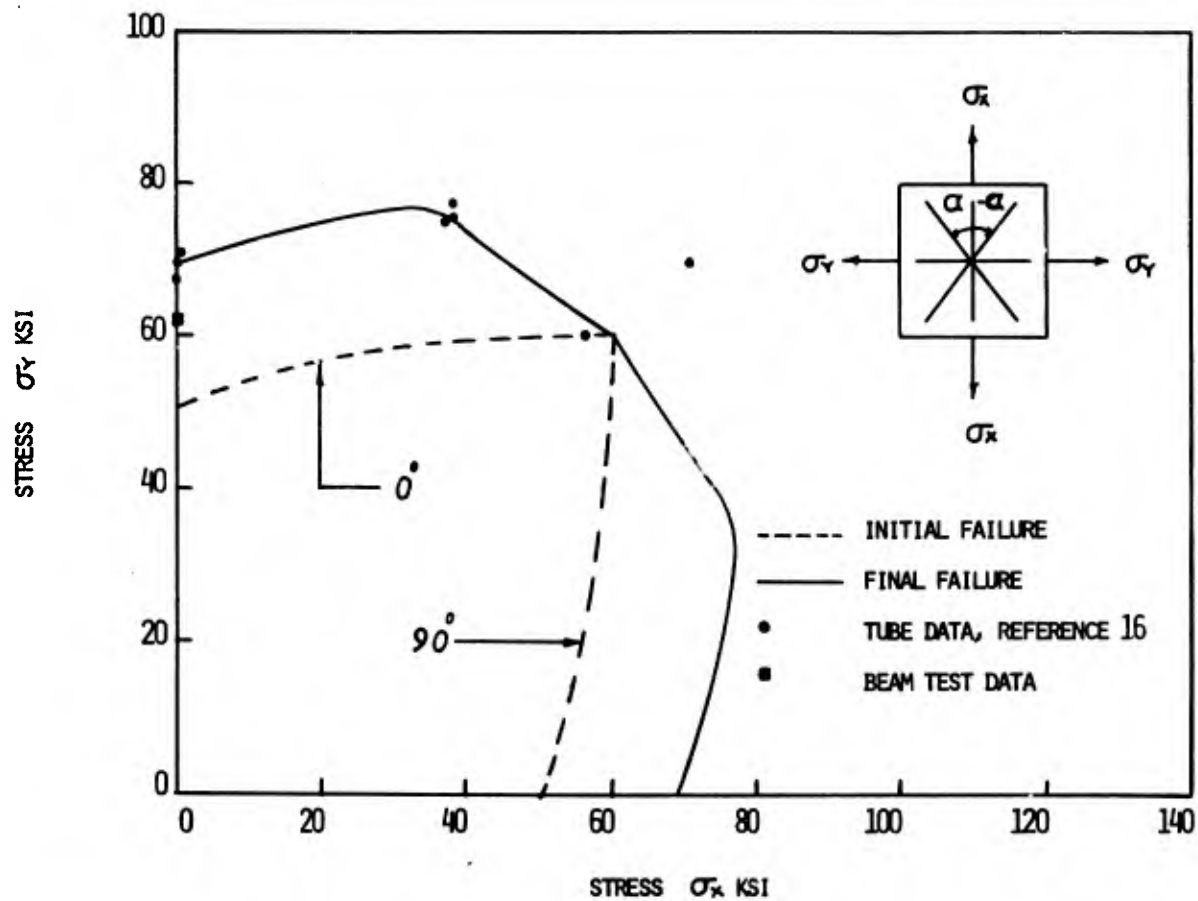


Figure 31. Strength Envelope for $(0^\circ/\pm 45^\circ/90^\circ)_s$ Laminate

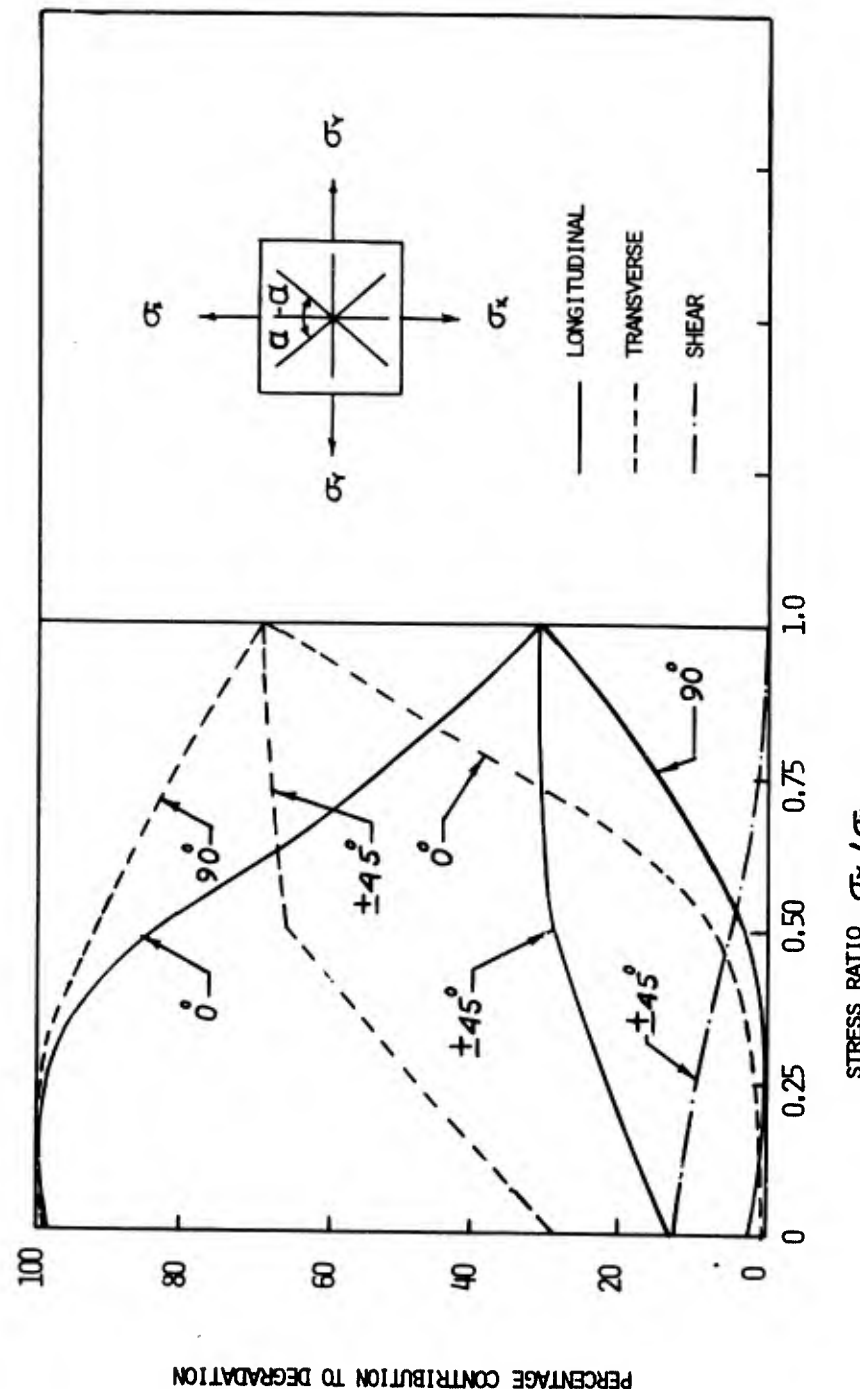


Figure 32. Percentage Contribution to Degradation of $(0^\circ/\pm 45^\circ/90^\circ)_s$ Laminate Subjected to Various Stress Ratios

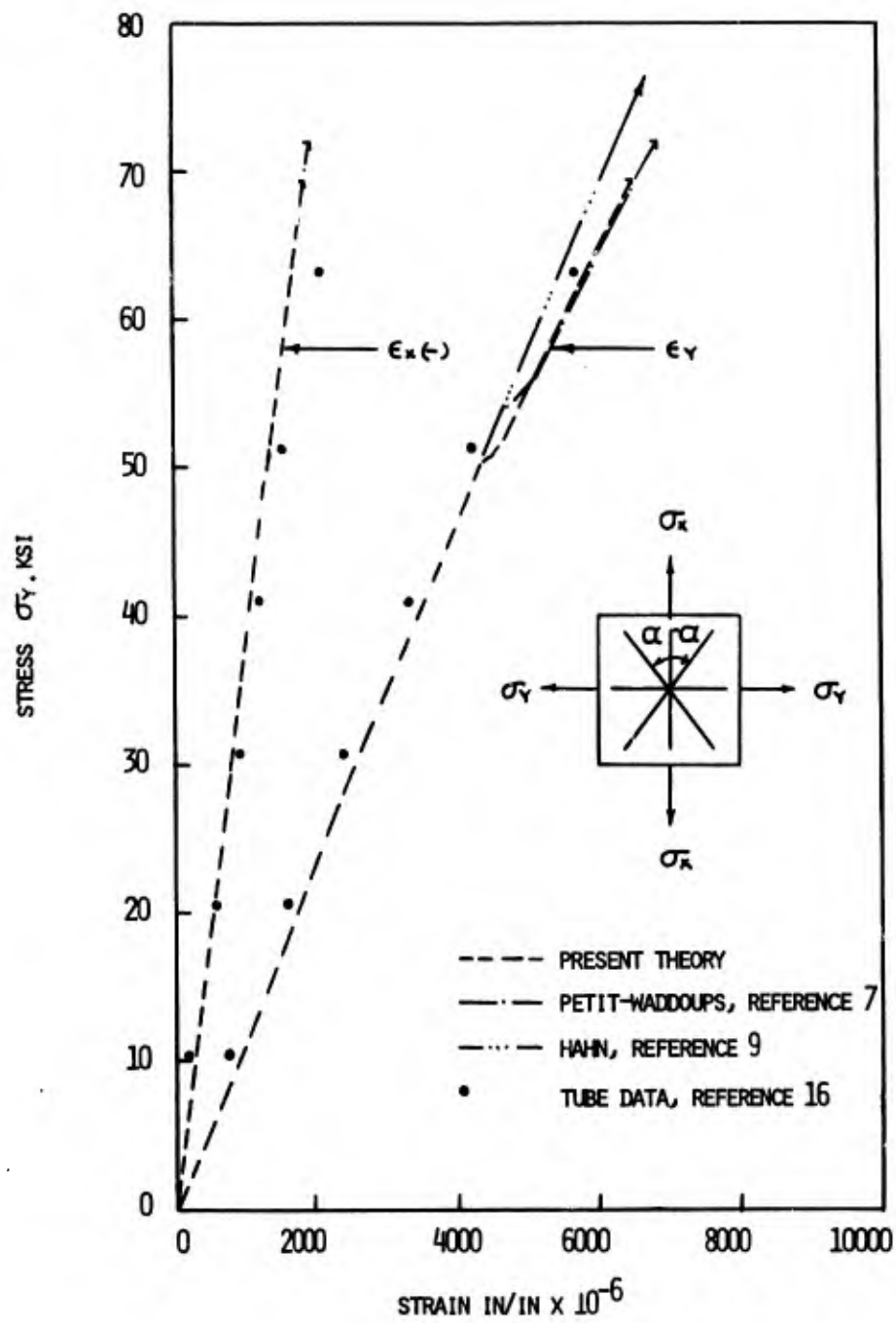


Figure 33. Stress-Strain Response of $(0^\circ/\pm 45^\circ/90^\circ)_s$ Laminate Subjected to Stress σ_y Only

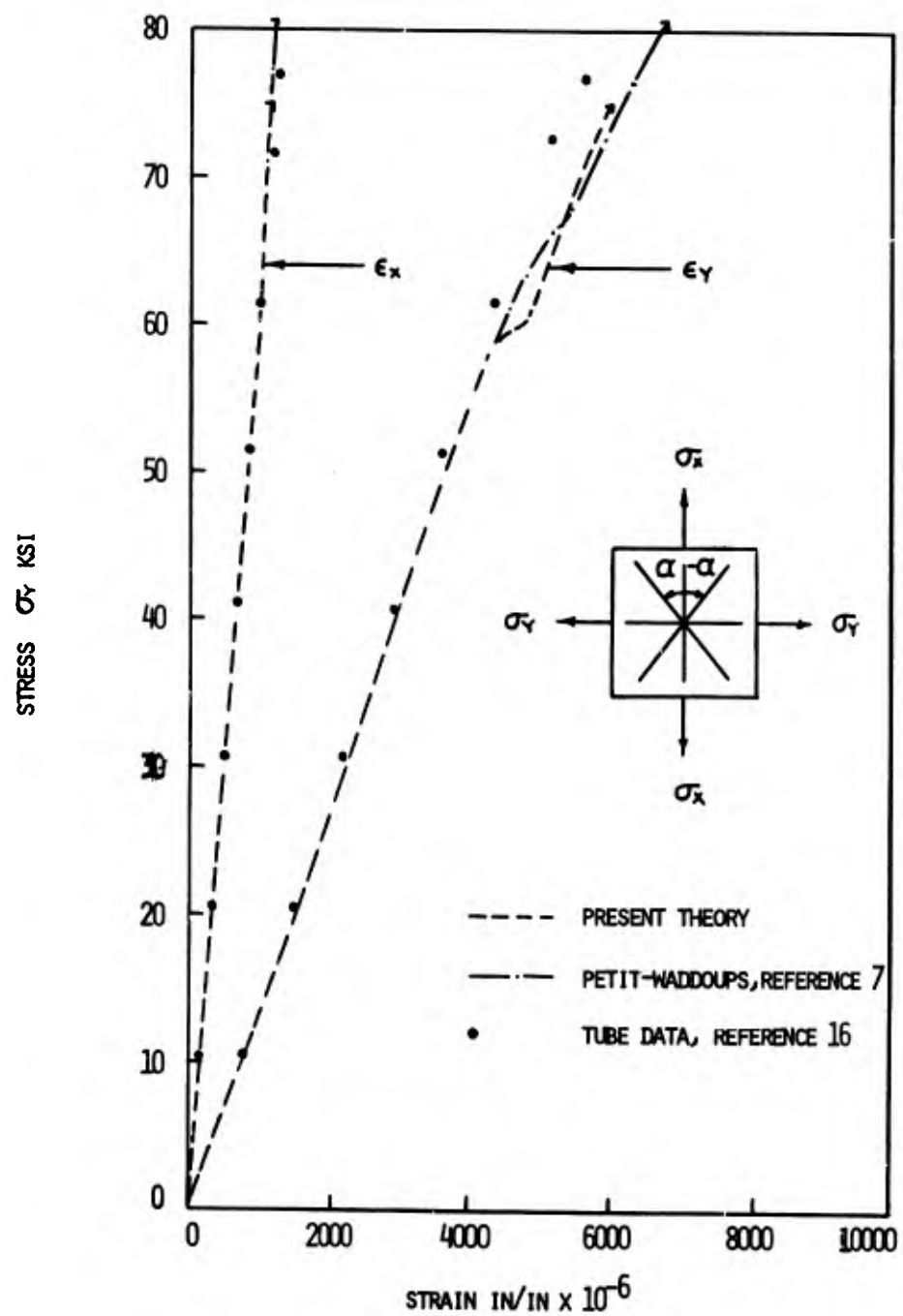


Figure 34. Stress-Strain Response of $(0^\circ/\pm 45^\circ/90^\circ)_s$ Laminate
Subjected to a Stress Ratio, $\sigma_x/\sigma_y = 1:2$

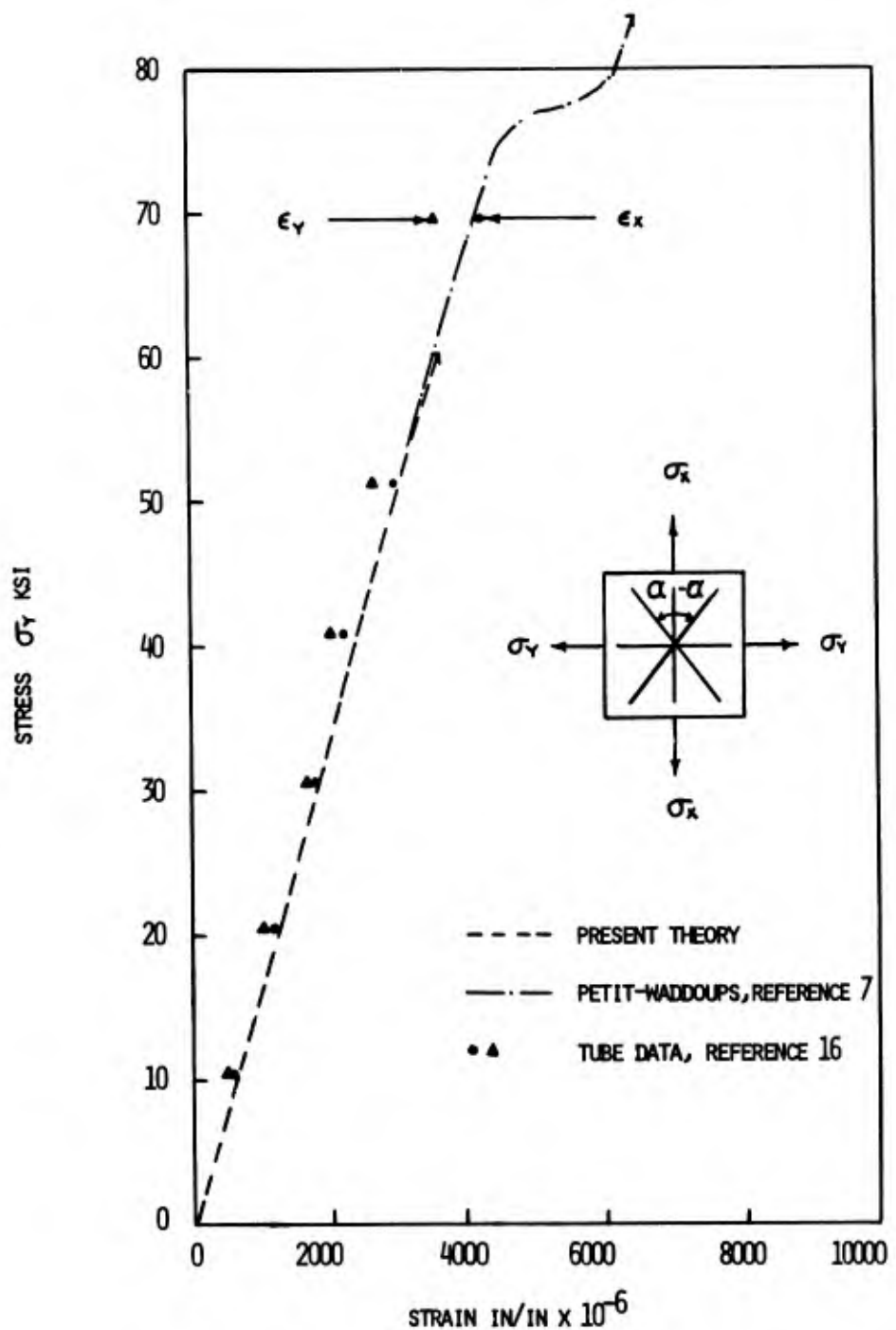


Figure 35. Stress-Strain Response of $(0^\circ/\pm 45^\circ/90^\circ)_s$ Laminate
Subjected to a Stress Ratio, $\sigma_x/\sigma_y = 1:1$

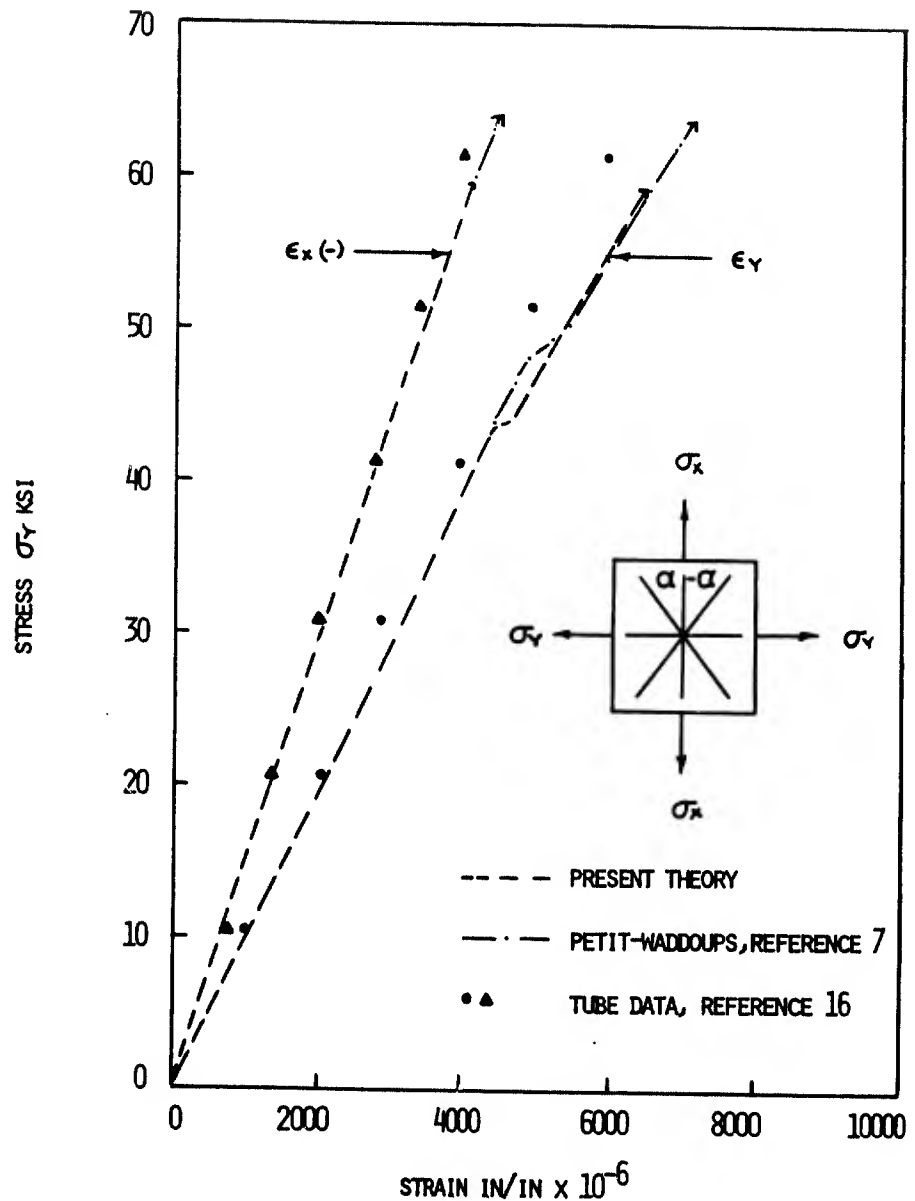


Figure 36. Stress-Strain Response of $(0^\circ/\pm 45^\circ/90^\circ)_s$ Laminate
Subjected to a Stress Ratio, $\sigma_x/\sigma_y = -1:2$

TABLE VI
FAILURE STRESSES AND PERCENTAGE DEGRADATION OF $(0^\circ/\pm 45^\circ/90^\circ)_s$ LAMINATE

No	Stress Ratio	Stresses, ksi			Initial/Final Failure			Percentage Degradation			Remarks		
		σ_x	σ_y	τ_{xy}	0° Plies			$\pm 45^\circ$ Plies					
					L	T	S	L	T	S	L	T	S
1	0 1 0	0	50.38	0	1.06	98.94	0	5.61	13.50	5.99	44.92	0.5	0
2	1 4 0	13.71	54.85	0	0.06	99.94	0	9.92	23.56	4.32	45.87	0.55	0
3	1 2 0	28.63	57.27	0	1.92	91.76	0	15.39	35.96	2.19	41.76	4.66	0
4	3 4 0	44.30	59.06	0	11.71	80.93	0	22.35	51.31	0.59	36.42	27.68	0
5	1 1 0	60.25	60.25	0	30.78	69.22	0	30.78	69.22	0	30.78	69.22	0
6	4 3 0	59.06	44.30	0	36.42	27.68	0	22.35	51.31	0.59	11.71	80.93	0
7	2 1 0	57.27	28.63	0	41.76	4.66	0	15.39	35.98	2.19	1.92	91.76	0
8	4 1 0	54.85	13.71	0	45.87	0.55	0	9.92	23.56	4.32	0.06	99.94	0
9	1 0 0	50.38	0	0	44.92	0.50	0	5.61	13.50	5.99	1.06	98.94	0
		69.38	0	0	98.88	1.12	0	12.45	29.29	12.17	2.34	98.94	0

L = Longitudinal; T = Transverse; S = Shear

TABLE VII
FAILURE STRESSES AND PERCENTAGE DEGRADATION OF $(0_2^0/\pm 45^0/90^0)_s$ LAMINATE

No	Stress Ratio	Stresses ksi			Initial/Final Failure			Percentage Degradation ksi			Remarks	
		$\sigma_x \sigma_y \tau_{xy}$			0° Plies			±45° Plies				
		σ_x	σ_y	τ_{xy}	L	T	S	L	T	S		
1	0 1 0	0	$\frac{43.94}{56.07}$	0	$\frac{0.42}{0.85}$	$\frac{99.58}{99.58}$	0	$\frac{7.61}{15.55}$	$\frac{18.19}{36.32}$	$\frac{5.19}{9.80}$	$\frac{45.71}{92.42}$	
2	1 4 0	23.69	$\frac{47.38}{62.36}$	0	$\frac{0.78}{0.94}$	$\frac{94.45}{94.45}$	0	$\frac{13.87}{28.83}$	$\frac{32.57}{65.02}$	$\frac{2.72}{6.15}$	$\frac{43.10}{94.55}$	
3	1 2 0	$\frac{31.18}{43.65}$	36.21	$\frac{48.28}{58.20}$	0	$\frac{4.51}{5.83}$	$\frac{87.71}{87.71}$	0	$\frac{17.46}{29.77}$	$\frac{41.24}{67.13}$	0	$\frac{39.75}{71.96}$
4	3 4 0	49.19	$\frac{49.19}{54.03}$	0	$\frac{11.65}{13.12}$	$\frac{80.94}{80.94}$	0	$\frac{22.31}{30.38}$	$\frac{51.22}{68.39}$	$\frac{0.59}{1.23}$	$\frac{36.43}{54.71}$	
5	1 1 0	$\frac{54.03}{67.06}$	67.06	$\frac{50.30}{50.30}$	0	$\frac{26.94}{26.94}$	$\frac{71.84}{71.84}$	0	$\frac{29.42}{29.42}$	$\frac{66.41}{66.41}$	$\frac{0.02}{0.02}$	$\frac{27.54}{30.88}$
6	4 3 0	71.25	$\frac{35.63}{41.35}$	0	$\frac{36.91}{53.78}$	$\frac{24.57}{32.02}$	0	$\frac{21.58}{30.42}$	$\frac{49.64}{68.44}$	$\frac{0.7}{1.14}$	$\frac{10.35}{13.63}$	
7	2 1 0	$\frac{82.71}{100.81}$	71.25	$\frac{17.81}{25.20}$	0	$\frac{44.27}{98.93}$	$\frac{0.50}{0.58}$	0	$\frac{12.63}{27.47}$	$\frac{29.76}{62.28}$	$\frac{3.21}{7.09}$	$\frac{32.02}{32.02}$
8	4 1 0	66.59	0	0	$\frac{45.41}{98.91}$	$\frac{0.49}{1.09}$	0	$\frac{5.75}{12.59}$	$\frac{13.82}{29.67}$	$\frac{6.02}{12.11}$	$\frac{0.21}{0.24}$	
9	1 0 0	$\frac{93.43}{100.81}$	66.59	0	0	0	0	0	0	$\frac{1.03}{2.26}$	$\frac{98.97}{98.97}$	

L = Longitudinal; T = Transverse; S = Shear

TABLE VIII
FAILURE STRESSES AND PERCENTAGE DEGRADATION OF $(0^\circ/\pm 45^\circ/0^\circ/90^\circ)_s$ LAMINATE

No	Stress Ratio	Initial/Final Failure				Percentage Degradation ksi				Remarks	
		Stresses ksi		0° Plies		$\pm 45^\circ$ Plies		90° Plies			
		σ_x	σ_y	τ_{xy}	L	T	S	L	T		
1	0 1 0	0	$\frac{34.19}{41.85}$	0	$\frac{0.42}{0.84}$	$\frac{99.58}{99.58}$	0	$\frac{7.61}{15.59}$	$\frac{18.20}{36.32}$	$\frac{5.18}{9.73}$	
2	1 4 0	$\frac{8.94}{11.24}$	$\frac{35.94}{44.96}$	0	$\frac{0.08}{0.24}$	$\frac{99.92}{99.92}$	0	$\frac{9.67}{20.26}$	$\frac{22.98}{46.70}$	$\frac{4.40}{8.99}$	
3	1 2 0	$\frac{18.72}{23.77}$	$\frac{37.44}{47.54}$	0	$\frac{0.05}{0.10}$	$\frac{97.97}{97.97}$	0	$\frac{12.02}{25.11}$	$\frac{28.38}{57.26}$	$\frac{3.48}{7.74}$	
4	3 4 0	$\frac{28.96}{36.18}$	$\frac{38.61}{48.24}$	0	$\frac{1.35}{1.42}$	$\frac{92.90}{92.90}$	0	$\frac{14.70}{29.04}$	$\frac{34.43}{65.33}$	$\frac{2.41}{5.63}$	
5	1 1 0	$\frac{39.79}{46.50}$	$\frac{39.79}{46.50}$	0	$\frac{4.59}{5.21}$	$\frac{87.56}{87.56}$	0	$\frac{17.81}{29.72}$	$\frac{41.36}{66.93}$	$\frac{1.48}{3.55}$	
6	4 3 0	$\frac{55.28}{58.61}$	$\frac{41.46}{43.96}$	0	$\frac{12.57}{12.71}$	$\frac{80.21}{80.21}$	0	$\frac{22.80}{30.35}$	$\frac{52.28}{68.35}$	$\frac{0.52}{1.30}$	
7	2 1 0	$\frac{77.92}{82.90}$	$\frac{38.96}{41.45}$	0	$\frac{33.51}{39.20}$	$\frac{48.19}{53.29}$	0	$\frac{26.84}{30.72}$	$\frac{60.96}{69.10}$	$\frac{0.13}{0.18}$	
8	4 1 0	$\frac{78.13}{100.91}$	$\frac{19.53}{25.23}$	0	$\frac{43.78}{98.01}$	$\frac{1.00}{1.38}$	0	$\frac{13.17}{28.63}$	$\frac{31.00}{64.70}$	$\frac{2.95}{6.67}$	
9	1 0 0	$\frac{70.54}{100.40}$	0	0	$\frac{44.93}{97.85}$	$\frac{0.96}{2.15}$	0	$\frac{3.97}{8.61}$	$\frac{9.61}{20.52}$	$\frac{0.41}{0.57}$	
										$\frac{2.00}{4.45}$	
										$\frac{98.00}{53.00}$	
										0	

L = Longitudinal; T = Transverse; S = Shear

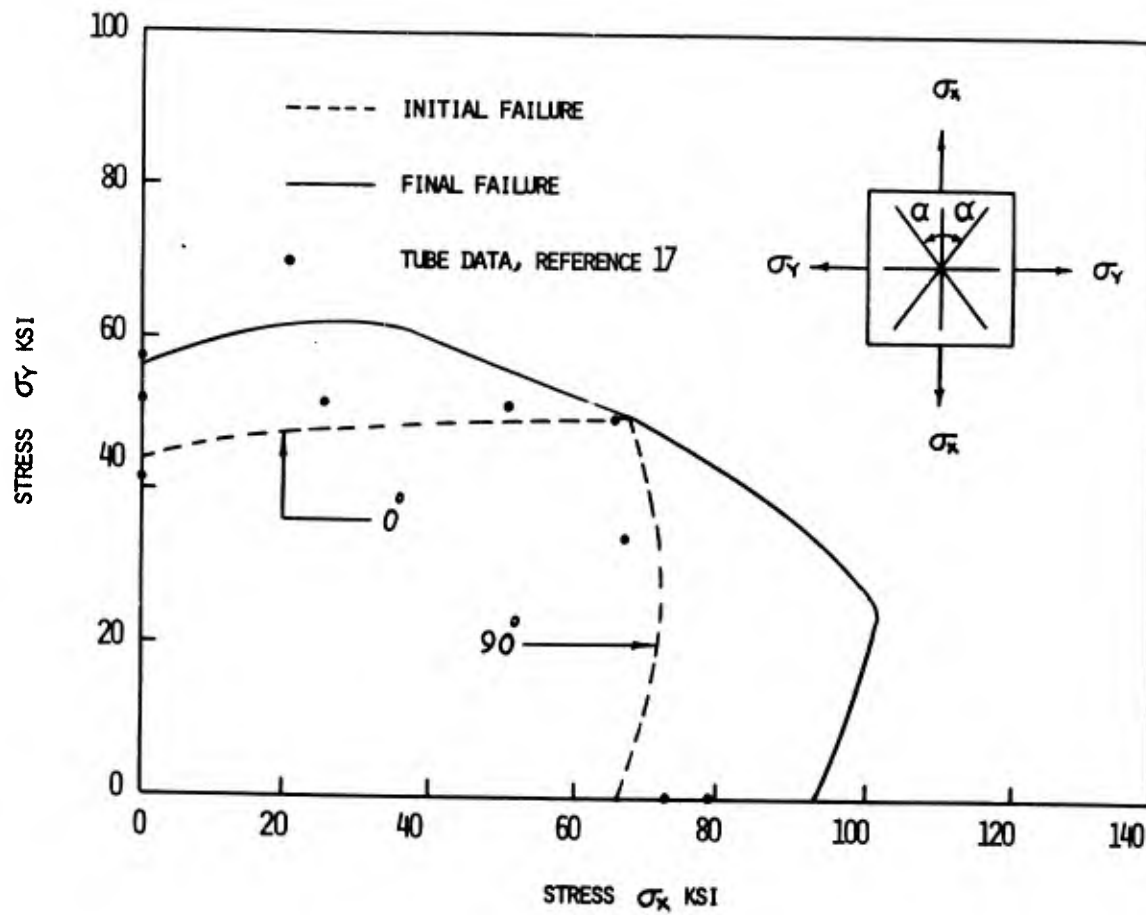


Figure 37. Strength Envelope for $(0^\circ/\pm 45^\circ/90^\circ)_s$ Laminate

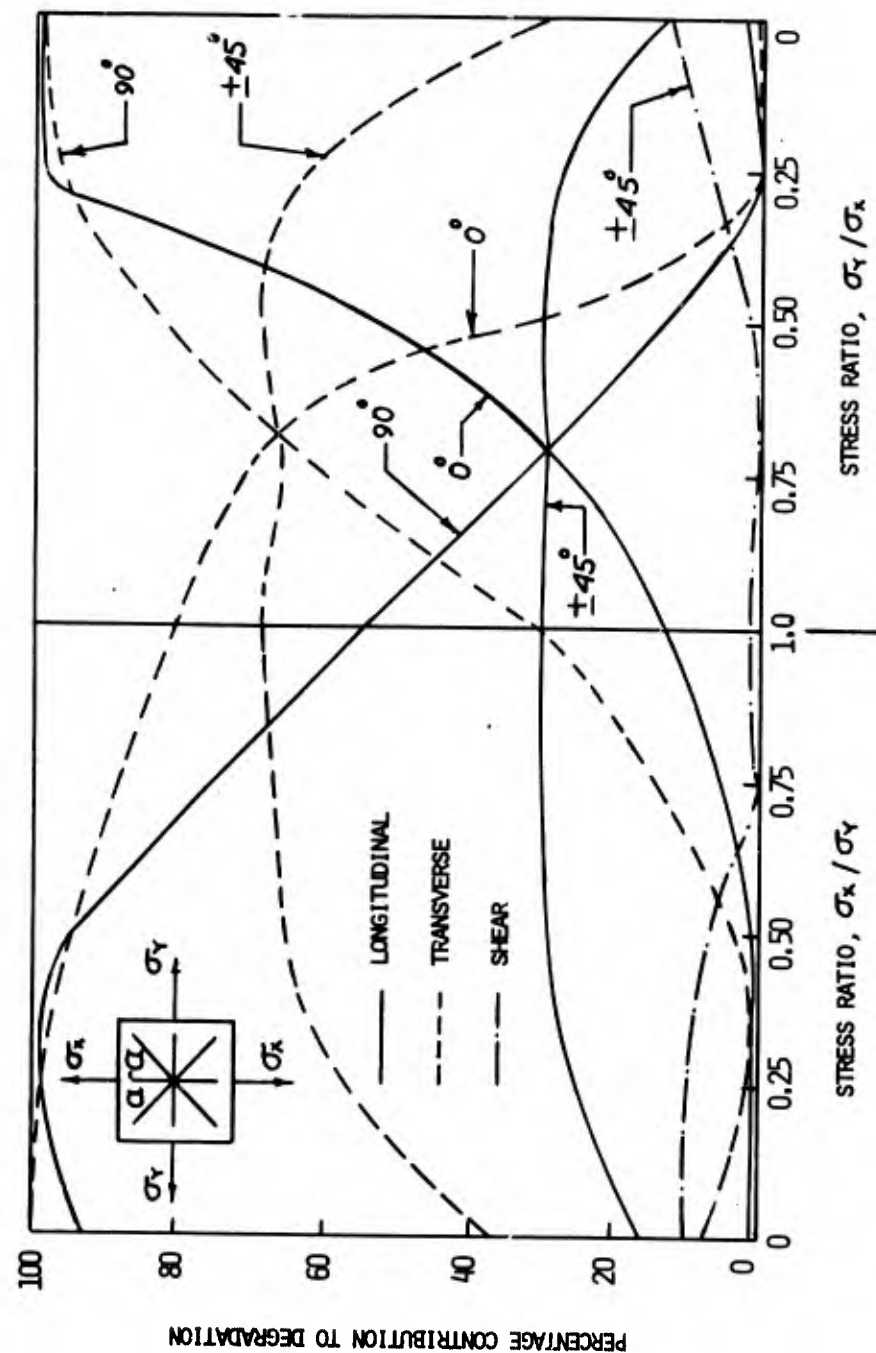


Figure 38. Percentage Contribution to Degradation of $(0^\circ/\pm 45^\circ/90^\circ)_s$ Laminate Subjected to Various Stress Ratios

Figures 39 and 40 show the theoretical strength envelope and contributions to degradation of $(0^\circ/\pm 45^\circ/0^\circ/90^\circ)_s$ laminate. The experimental data available for this laminate is quite meager (Reference 16). The comparison of this with analytical data (Table IX) indicates good corroboration for stress ratios $\sigma_x/\sigma_y/\tau_{xy}$ of 1:0:0, 0:0:1, 1:2:1, but far from satisfactory correlation for the stress ratio σ_x/σ_y of 1:2.

Strength envelopes of three $(0^\circ/\pm 45^\circ/90^\circ)$ family laminates are shown in Figure 41. The figure indicates that the laminate increases in strength for certain stress ratios due to percentage increase of 0° plies, but decreases in strength for other stress ratios.

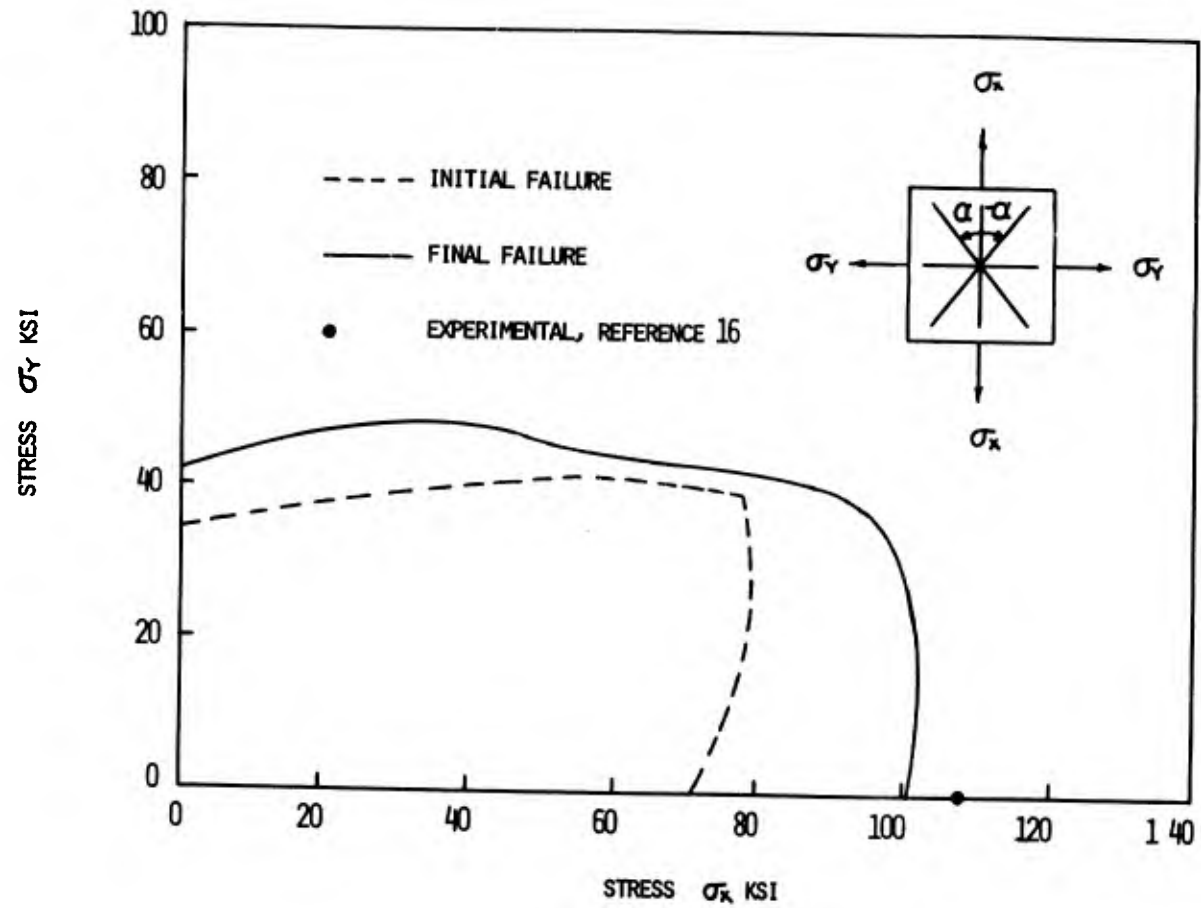


Figure 39. Strength Envelope for $(0^\circ/\pm 45^\circ/0^\circ/90^\circ)_s$ Laminate

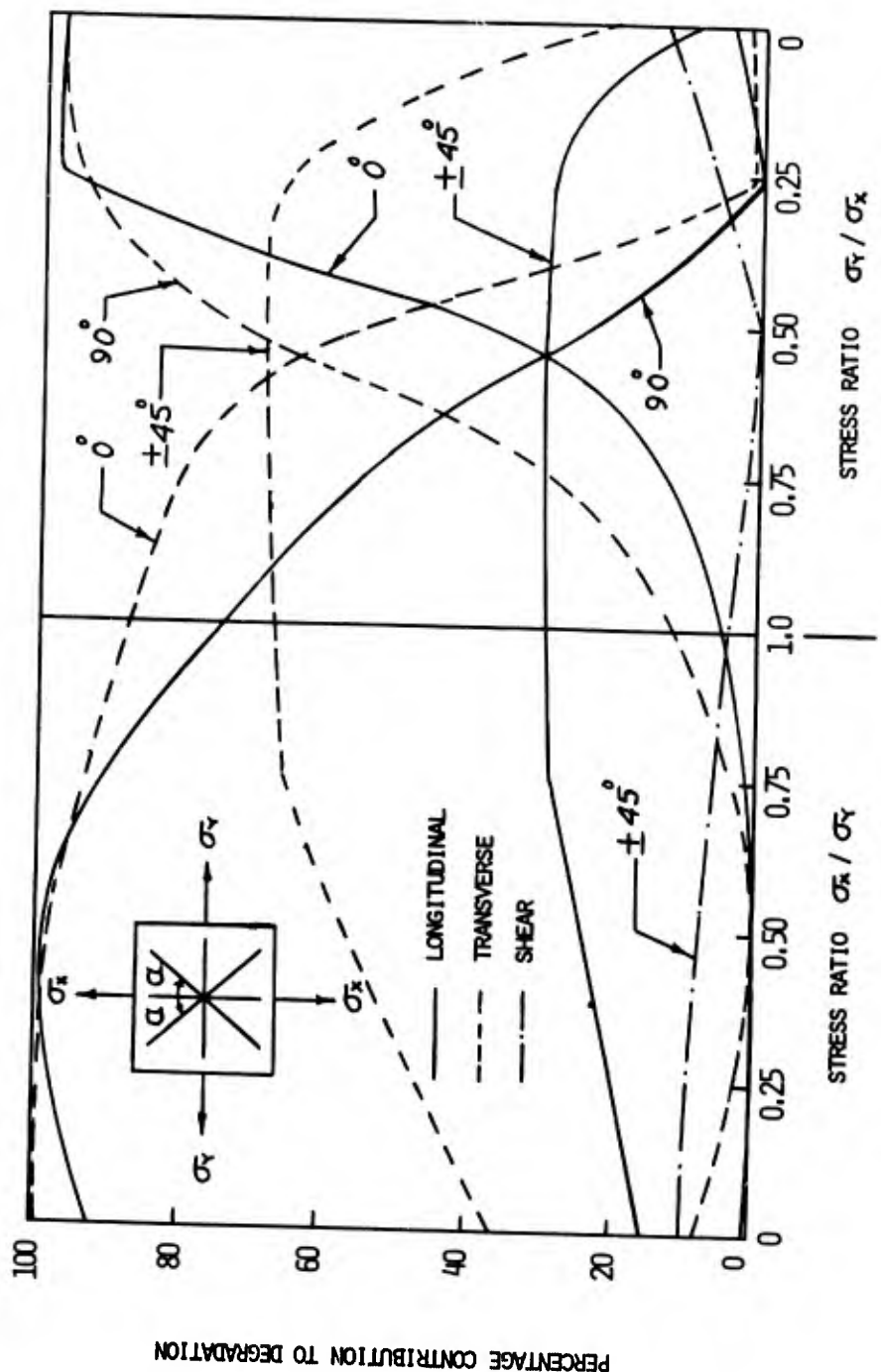


Figure 40. Percentage Contribution to Degradation of $(0^\circ/+45^\circ/0^\circ/90^\circ)_s$ Laminate Subjected to Various Stress Ratios

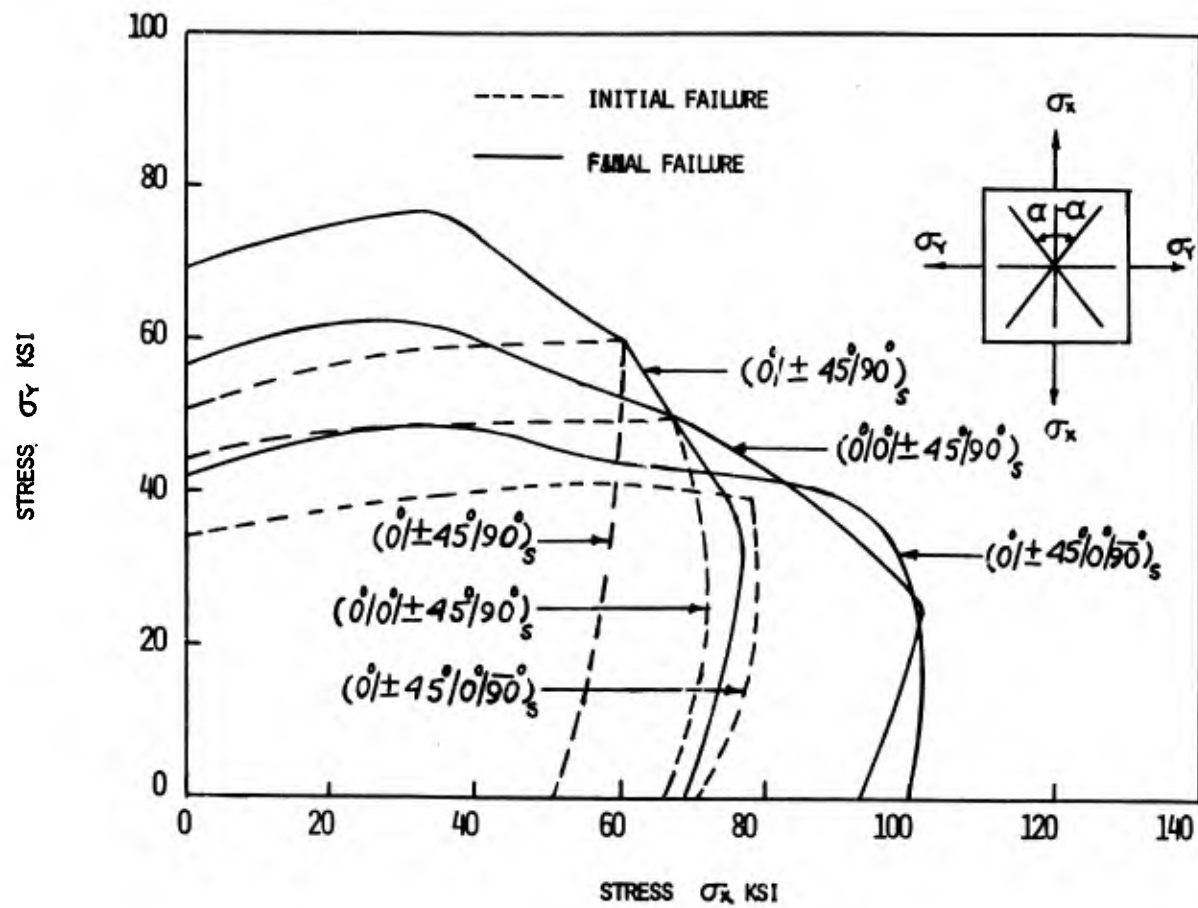


Figure 41. Strength Envelopes of $(0^\circ/\pm 45^\circ/90^\circ)_s$ Laminates

TABLE IX
ANALYTICAL-EXPERIMENTAL STRENGTHS OF $(0^\circ/\pm 45^\circ/0^\circ/\overline{90^\circ})_s$ LAMINATE

Method of Testing	Stress Ratio			Analytical Stresses in KSI			Experimental Stresses in KSI		
	σ_x	σ_y	τ_{xy}	σ_x	σ_y	τ_{xy}	σ_x	σ_y	τ_{xy}
Bear. Method	1	0	0	104.4	0.	0.	107.6	0.	0.
Tube	0	0	1	0.	0.	35.55	0.	0.	36.28
Tube	.1	2	1	20.91	41.83	20.91	17.8	34.5	17.8
							18.6	36.9	18.6
							20.4	39.3	20.4
Tube	1	2	0	23.77	47.54	0.	37.4	74.8	0.
							43.4	86.7	0.
							44.0	89.6	0.

SECTION V

DISCUSSION OF RESULTS AND CONCLUSIONS

In Section II, we presented a technique for predicting the response of composite laminates. The incremental constitutive law defining the nonlinear behavior of anisotropic materials is specialized for orthotropic laminas under plane stress conditons. Using simplifying assumptions, we extended the use of the incremental constitutive law to the analysis of multidirectional laminates subjected to inplane loads. In the application of the technique, we represented the nonlinearity of basic stress-strain curves of laminas by the use of cubic spline interpolation functions.

The incremental constitutive law in conjunction with the failure criterion was used to predict the response of various boron-epoxy laminates. The available experimental data was not only compared with the predictions based upon the present theory, but also with theoretical results obtained using techniques of Petit-Waddoups and Hahn. In the case of unidirectional laminates subjected to biaxial stress states, we could make no comparison because no relevant experimental data was available.

The study of other laminates revealed that the boron-epoxy material system tends to retain its orthotropic characteristics to failure. Up to the point of experimental failure, experimental stress-strain curves matched analytical curves based upon present theory more closely than the curves using the techniques of References 7 to 9. However, in the case of the $(0^\circ/\pm 60^\circ)_s$ laminate subjected to the stress σ_y , considerable deviation between experimental and analytical results was observed. The probable cause is traceable to the role played by the 0° plies in the laminate; we assumed that transverse degradation does not precipitate a total failure since the plies are still capable of sustaining longitudinal loads. This is probably not realized, and the 0° plies may lose their total effectiveness on transverse impairment. This behavior of

0° plies in the boron-epoxy laminate is quite different from that observed in a glass-epoxy laminate (Reference 18).

No experimental data is available for the $(0^\circ/\pm 45^\circ)_s$ laminate. In light of the behavior of $(0^\circ/\pm 60^\circ)_s$ laminate, however, we expect that the transverse degradation of 0° plies would precipitate general failure of 0° plies and the laminate.

This study has shown that the incremental constitutive law in combination with the failure criterion proposed in this report provides a suitable analytic means for predicting the behavior of laminates under general states of stress using only the unidirectional laminate property data obtained under simple load conditions. Though attention was confined to the tension-tension quadrant of the stress space, the technique is general and holds for other quadrants as well, provided no buckling occurs. It has also demonstrated that a need exists for improving the experimental techniques to generate good data to clarify fuzziness that exists between analytic and experimental responses.

REFERENCES

1. Structural Design Guide for Advanced Composite Applications, 3rd Ed., January 1973, Advanced Composites Division, AF Materials Laboratory, Wright-Patterson AFB, Ohio.
2. R. S. Sandhu, A Survey of Failure Theories of Isotropic and Anisotropic Materials, AFFDL-TR-72-71, January 1972, Wright-Patterson AFB, Ohio, AD756889.
3. S. W. Tsai, Strength Characteristics of Composite Materials, NASA CR-224, April 1965.
4. S. W. Tsai, D. F. Adams and D. R. Doner, Analysis of Composite Structures, NASA CR-620, November 1966.
5. J. V. Noyes, and B. H. Jones, Crazing and Yielding of Reinforced Composites, AFML-TR-68-51, March 1968.
6. K. D. Chiu, "Ultimate Strengths of Laminated Composites," Journal of Composite Materials, Vol 3, p 578, July 1969.
7. P. H. Petit and M. E. Waddoups, "A Method of Predicting the Non-Linear Behavior of Laminated Composites," Journal of Composite Materials, Vol 3, page 2, January 1969.
8. Hong T. Hahn and Stephen W. Tsai, "Nonlinear Elastic Behavior of Unidirectional Composite Laminae," Journal of Composite Materials, Vol 7, pp 102-108, January 1973.
9. H. T. Hahn, "Nonlinear Behavior of Laminated Composites," Journal of Composite Materials, Vol 7, pp 257-271, April 1973.
10. T. H. Lin, D. Salinas, and Y. M. Ito, "Effects of Hydrostatic Stress On the Yielding of Cold Rolled Metals and Fiber-Reinforced Composites," Journal of Composite Materials, Vol 6, pp 409-413, July 1972.
11. E. L. McKague, G. H. Lemon and B. E. Kaminski, Development of Engineering Data for Advanced Composite Materials, AFML-TR-70-108, Vol 1, AF Materials Laboratory, Wright-Patterson AFB, Ohio.
12. A. Ralston and H. S. Wilf, Mathematical Methods for Digital Computer, Volume II, John Wiley and Sons, Inc, New York.
13. J. L. Walsh, J. H. Ahlberg, E. N. Nilson, "Best Approximation Properties of the Spline Fit, Journal of Mathematics and Mechanics, Vol II, No. 2, pp 225-233, 1962.
14. "Filamentary Composite Laminates Subjected to Biaxial Stress Fields," Contract F33615-70-C-1298, Fourth Quarterly Progress Report, IIT Research Institute/General Dynamics, Ft Worth, March 1971.

15. B. W. Cole and R. B. Pipes, Utilization of the Tubular and Off-Axis Specimens for Composite Biaxial Characterization, AFFDL-TR-72-130, Proceedings of Conference held at Dayton, Ohio 26-28 Sep 72.
16. Advanced Composite Wing Structures, Boron-Epoxy Design Data, Vol III-Experimental Data, Contract F33615-68-C-1301, Technical Report AC-SM-ST-8085, Vol III, Grumman Aerospace Corp, November 1969.
17. C. L. Stotler, D. J. Van Putten and E. O. Dickerson, Boron/Epoxy Wing Skins F-100D Aircraft Structural Design and Analysis, North American Rockwell Corp., Technical Report AFML-TR-71-29, Vol I, August 1971.
18. R. S. Sandhu, J. B. Monfort, F. E. Hussong, and E.E. Zink, Laminate Tubular Specimens Subjected to Biaxial Stress States (Glass-Epoxy) Technical Report AFFDL-TR-73-7, Vol 1, Feb 1973, Wright-Patterson AFB, Ohio. AD908917.